Stony Brook University

Role of a metabolic burst and titration of an unstable activator in the entrainment of division to growth

A Dissertation Presented

by

Lucas Carey

to

The Graduate School

in Partial Fulfillment of the

Requirements

for the Degree of

Doctor of Philosophy

in

Genetics

Stony Brook University

May 2010

Stony Brook University

The Graduate School

Lucas Carey

We, the dissertation committee for the above candidate for the Doctor of Philosophy degree, hereby recommend acceptance of this dissertation.

Bruce Futcher, Dissertation Advisor
Professor, Department of Microbiology and Genetics

Aaron Neiman
Associate Professor, Department of Biochemistry and Cell Biology

Rolf Sternglanz
Professor, Department of Biochemistry and Cell Biology

Robert Haltiwanger, Outside Examiner
Professor, Department of Biochemsitry and Cell Biology

John Reinitz
Professor, Department of Applied Math and Statistics
Stony Brook University

This dissertation is accepted by the Graduate School.

Lawrence Martin
Dean of the Graduate School

Abstract of the Dissertation

Role of a metabolic burst and titration of an unstable activator in the entrainment of division to growth

By

Lucas Carey

Doctor of Philosophy

in

Genetics

Stony Brook University

2010

Most cells coordinate increase in mass with an increase in cell number. Using simulations I show that exponentially growing cells require size control (a molecular link between growth and division) to maintain a population with a biologically reasonable cell size distribution, though linearly growing cells do not. The main regulator of cell-cycle commitment in budding yeast is the G1 cyclin Cln3, which partners with the Cyclin Dependent Kinase (CDK) Cdc28 to activate the transcription factor SBF and promote transcription of over 150 genes involved in cell-cycle progression. Commitment to Start (passage from G1 into S) involves transition from a low Cyclin/CDK state to a high Cyclin/CDK state, and this transition is driven largely by Cln3/CDK activity. Cln3 is recruited indirectly to DNA by SBF where it both activates transcriptional activators and inhibits transcriptional repressors. Cln3 is unstable, so the amount of Cln3 in cells is proportional to their size (biosynthetic capacity). By measuring cell volume throughout the cell-cycle we show that addition of more SBF binding sites increases cell size, and that this increase varies depending on the genetic dose of CLN3. This suggests that cells may measure size by titrating an unknown and noisy amount of Cln3 protein to a known and constant number of SBF binding sites. Slowly growing cells produce less cyclin protein per unit mRNA than do rapidly growing cells. Using a genetic system in which I

can tightly control the level of cyclin expression I show that slowly growing cells require less cyclin expression to pass through Start; this growth dependent threshold requirement may be a result of the instability of Cln3. Finally, I show that in addition to the transcriptional positive feedback loop that switches cells from low Cln/CDK to high Cln/CDK, there may be contribution from a metabolic feedback loop in which Cyclin/CDK activity may drive, and be driven by, metabolic changes during Start. These metabolic changes involve the sudden conversion of stored carbohydrate (glycogen and trehalose) to glucose in late G1 phase. I show that carbohydrate mutants have cell-size phenotypes, that genes involved in carbohydrate metabolism are CDK targets and that genes involved in cell-cycle control are Protein Kinase A (PKA) targets. I show that there is a spike in PKA activity around Start, and that the transcriptional profile around Start in ethanol grown cells is similar to that of ethanol grown cells spiked with glucose. These results suggest that slowly growing carbon-deprived cells briefly become rapidly growing carbon-rich cells around Start, and this increase in biosynthetic capacity may drive cells through Start.

Table of Contents

List of Abbreviations

Full Name / Description	Abbreviation
Cyclin Dependent Kinase	CDK
cyclic AMP	cAMP
Protein Kinase A (cAMP dependent kinase)	PKA
Glycogen Phosphorylase	Gph1
Glycogen Synthase 2	Gsy2
Neutral Trehalase	Nth1
[cAMP] Phosphodiestersase 2	Pde2
SCB Binding Factor (Swi4 + Swi6)	SBF
MCB Binding Factor (Mbp1 + Swi6)	MBF
Swi4/6 Cell cycle Binding element (CRCGAAA)	SCB
MluI Cell cycle Binding element (ACGCGT)	MCB
Fluorescence Resonance Energy Transfer	FRET
Glycogen Binding Domain	GBD
Nuclear Localization Signal	NLS
Yeast extract Peptone +2% Dextrose	YPD
Yeast extract Peptone + 2% Ethanol	YPE
Synthetic Complete media	SC

List of Figures

List of Tables

Chapter 1. Introduction

Growth of any cell population involves both increase in mass (the cell growth cycle) and an increase in cell number (the cell division cycle). There are two very old and fundamental questions that center around these two cycles. The first is the search for the mechanisms that drive each cycle; the second for the mechanisms that couple growth and division cycles. Based on the observation that a growing population of cells in a constant environment maintains size homeostasis, intuitively there are two options: either the two cycles are completely independent but perfectly synchronized, or that the two cycles interact and regulate each other. If the growth cycle were only slightly longer than the cell division cycle, cells in the population would become infinitely small, and if the reverse were true, if the growth cycle were slightly shorter than the division cycle, cells would become infinitely large. My research focuses on the molecular links between the two cycles, and on the role of metabolism in regulating Start in slowly growing cells.

1.1 Experimental outline

Start involves the transcriptional activation of over 100 genes involved in DNA replication, budding, and the switch from G1 into S and commitment to cell-cycle progression. Two genes activate this burst of transcription: the G1 cyclin Cln3 and the mysterious protein Bck2. Cln3 and Bck2 act independently through the transcription factors SBF and MBF to promote Start, and a *cln3 bck2* double mutant is dead because it fails to activate the transcription of *CLN2*. I began my PhD research looking for genetic suppressors of *cln3 bck2* lethality. While the screen missed the major suppressor, Whi5, because the gene was not in the library, I identified a few genes involved in histone modifications (Stb1, Sin3, Rpd3). Mutants in these genes partially derepress *CLN2* transcription; these genes are probably involved in maintaining the *CLN2* promoter in an off state, but Stb1 may also be a transcriptional activator (Costanzo, Schub et al. 2003). Hongyin Wang and I showed that *bck2 whi5* mutants are responsive to *CLN3* expression, but *bck2 whi5 stb1* mutants are not, suggesting that Whi5 and Stb1 act in concert to repress *CLN2* in G1 prior to Start. This work is published (Wang, Carey et al. 2009).

During her rotation Ying Cai showed that a high-copy plasmid containing four tandem binding sites for SBF (4xSCB) increases the critical size for passage through Start. Ms. Cai, Dr. Wang and I showed that ability of extra SCBs to increase cell size is due to titration of the G1 cyclin Cln3; the 4xSCB plasmid has no affect in cells containing two genomic copies of *CLN3*. We also showed that, in addition to the activator Cln3, the plasmid titrates out the repressors of SBF, Whi5 and Stb1; the 4xSCB plasmid makes *cln3* cells smaller (due to titration of the repressor) and has no affect in *cln3 whi5 stb1* cells. This work was published in the same paper (Wang, Carey et al. 2009) and will not be further discussed.

Following the identification of Whi5 as the major suppressor of *cln3 bck2* lethality I had to choose another project. I decided to look at the effect of storage carbohydrate liquidation on cell-cycle commitment in yeast growing on non-fermentable carbon. There were some very interesting and mostly overlooked papers showing that carbon starved yeast build large stores of storage carbohydrates during G1, only to metabolize them all in a fermentative burst around Start (Kuenzi and Fiechter 1969; Kuenzi and Fiechter 1972). This seemed like an odd thing for carbon-starved cells to do; if the glycogen stores were built up in case of starvation, we would expect the cell to keep them. We wondered if the liquidation of storage carbohydrates might be playing a role in Start. Cells growing in a glucose-limited chemostat undergo a spike in cAMP levels around Start (Muller, Exler et al. 2003), which may be indicative, and causative, of a metabolic and glycolytic burst. I found that carbohydrate null mutants have a larger critical size, that cells with increased glycogen synthase are smaller, and that a spike in cAMP can promote Start. I also found that both PKA responsive and glucose induced but PKA independent genes are transcriptionally activated around Start, and that a spike in cAMP can cause a burst in the growth rate around Start. These data suggest, but do not prove, that carbohydrate liquidation and the burst in cAMP around Start in ethanol grown cells turn slowly growing cells into quickly growing cells. I suggest that this helps cells reach a critical level of Cln protein production and aids in their progression through Start.

Exact measurements of glycogen and cAMP levels are tedious and require large numbers of cells. Even then, the numbers produced vary greatly from lab to lab. I set out to build fluorescent reporters for glycogen and for PKA activity in yeast. I cloned the AKAR3 FRET based PKA reporter (Allen and Zhang 2006) into a yeast expression vector and used it to confirm that single cells exhibit a spike in PKA activity around Start. I also developed a construct for detection of glycogen that relies on competition between a glycogen binding domain and a nuclear localization signal. Both constructs appear to be working but require more testing.

Finally, there has been some debate in the literature recently about the nature of growth (linear vs exponential) (Goranov, Cook et al. 2009) and the sizer and timer models of control of Start (Laabs 2003). I wrote a program that builds a population of yeast, in silico, in which the type of growth and control over Start can be altered. This allows me to ask what a population of cells with and without size control looks like, and how populations under different growth regimes behave. I find that if the exponential growth model is correct cells must have size control. While I am not the first to point this out (Cooper 2006), the ability to simulate and investigate growth dynamics in a population of single cells forces us to define, and allows us to check, some of our assumptions about growth and division by fitting the simulated cells to real cells.

1.2 Background

1.2.1 Early evidence for an energetic link between growth and division

The idea that cells need to grow large enough before dividing was first proposed by Richard Hertwig. In two papers from 1903 & 1908 based on work in sea urchins, he argued that growth alters the nucleo/cytoplasmic ratio, which brings about "tension" leading to cell division and restoration of the ideal ratio (reviewed in (Prescott 1976)). Early experiments (Hartmann 1926; Hammerling 1953; Prescott 1955; Prescott 1956; Prescott 1956; Prescott) using protozoa found that cell division can be delayed when pieces of the cytoplasm were removed, showing that while the nucleus controlled morphology (Hammerling), accumulation of something cytoplasmic was required for

division. Division can be inhibited by removal of cytoplasm until immediately before prophase (Mazia 1956) after which point the amoeba completes mitosis despite removal of cytoplasm. “Each operation results in a reversion for the cell to an earlier point of the cell life cycle” (Prescott 1976). The reverse experiment, in which cytoplasm was added and cell division was accelerated, was also done (Weisz 1956). Early researchers, though they believed in some form of size control, also realized that that this critical size is smaller that the size at which the majority of cells divide (Prescott 1955; Prescott 1956; Prescott 1956).

While the evidence that mitosis was controlled, or at least influenced, by cell size was very convincing, it was obvious early on that growth could not be the only thing controlling cell division, and that a special type of growth, or accumulation of something that does not accumulate during quiescent growth, was necessary for cell division. When Suctorian ciliates are fed only *Tetrahymena* they grow, but do not divide, and reach very large sizes. Then when the ciliates are fed purines and pyrimidines, or even their analogs, the ciliate commences mitosis (Wagtendonk 1955). This suggests that, while growth is a prerequisite for division there are other, more specific, nutritional requirements as well.

There was also early evidence that, while cytoplasmic growth was required for cell division, the amount of growth required was set by something nuclear, most likely the number of chromosomes. By altering ploidy in budding yeast, Robert Mortimer (Mortimer 1958) and others (Burns 1956) showed that over a six-fold increase in the number of chromosomes the cell division rate remains constant, and the cell growth rate increases so that the population maintains size homeostasis. Similar results were shown for tumor cells (Hsu 1954).

The link between growth and an energetic requirement for mitosis (the only visible part of the cell cycle at the time) became clear at around the same time. Removal of oxygen or addition of respiratory inhibitors applied during, or immediately before mitosis do not affect that mitosis, but inhibit the next division (Blumenthal 1930; Bullough and Johnson 1951). These results suggested that energy for division must be built up before

cells enter prophase, but that in prophase cells have enough energy to complete mitosis. Results like this suggested the requirement for a buildup of some sort of "energy reservoir" (reviewed in (Swann 1957; Swann 1958)) that builds up in interphase via glycolysis, and is metabolized prior to mitosis to provide energy for cell division. While early investigators could only guess at the molecular mechanisms involved, the idea that cells need to build up enough "initiation potential" (Cooper 1979) is an old one.

1.2.2 Identification of two points of cell-cycle commitment in G1

Among the approximately fifty genes found by Hartwell and colleagues in the *cdc* screen (Hartwell, Culotti et al. 1974) they identified two different classes of mutants that arrest as unbudded G1 cells. Class I mutants arrest identically to nitrogen starved cells (Byers and Goetsch 1974; Byers and Goetsch 1975; Johnston, Pringle et al. 1977) and are competent to mate upon release. Class I mutants arrest with an unduplicated spindle pole body and, unique among all CDC genes, do not increase in volume following arrest (Reed 1980). Class I arrested mutants, when shifted to nitrogen free media undergo nutrient arrest. Class II genes arrest like mating pheromone arrested cells, unbudded and with duplicated spindle pole bodies, and continue to grow in size. Unlike Class I, Class II mutants fail to arrest when nitrogen starved. These observations, along with several others, allowed Hartwell and colleagues to identify two points in G1 at which yeast make cell-cycle commitment decisions, Start A and Start B. In G1, prior to Start A, cells are sensitive to nutrient conditions, and will arrest if depleted for nitrogen, carbon, sulfate, biotin, and a subset of amino acids. After Start A, but before Start B, cells are no longer responsive to nutrient conditions, but are responsive to mating pheromone. Following Start B yeast will no longer shmoo in response to pheromone. When cells past Start B are challenged with pheromone or removal of an essential nutrient they fail to arrest until they have completed a mitotic cycle and are back in G1.

1.2.3 A requirement for *de novo* protein synthesis for cell-cycle progression

Prior to Start yeast can be considered undifferentiated, and can enter a nutritional arrest, mate, or initiate DNA replication. After Start, cells have activated Cdc28 and they are committed to a mitotic cycle. While neither cyclin (Evans, Rosenthal et al. 1983) nor the kinase activity of Cdc28 (Reed, Hadwiger et al. 1985) were known, it was immediately obvious that *de novo* synthesis each cell-cycle of Cdc28 was not required for cell-cycle progression (reviewed in Pringle and Hartwell, 1981). It was known that a threshold rate of protein synthesis was required to complete both Start (Jagadish and Carter 1977) and mitosis (Slater 1974). Yeast starved completely for nitrogen following Start fail to finish the cell cycle, but cells limited for nitrogen, so that protein synthesis is lessened but not prevented, prolong the budded phase. The periodically synthesized protein was most likely present in very low amounts at all points in the cell cycle; in analyses of 2D gels of protein synthesis during the cell cycle, no proteins were identified that changed in amount during the cell-cycle (Elliott and McLaughlin 1978). Early cell cycle researchers also realized that the unstable activator was also probably not a gene found in the *cdc* screen. Byers and Sowder (Byers and Sowder 1980) formed hybrid cells with *cdc* nuclei in wild-type cytoplasm. All tested mutants save for *cdc4* completed several cell-cycles at restrictive temperature, suggesting that all *CDC* gene products are present in excess, and not degraded each cell cycle. These results suggested that whatever was driving cells through the cell-cycle was unstable, synthesized discontinuously during the cell cycle, and not yet identified.

1.2.4 Identification of Cln3

In 1980 Bruce Carter and Peter Sudbery (Sudbery, Goodey et al. 1980) looked for small mutants, using alpha factor as an aid in the screen. They identified *WHI1-1*, a nonsense mutation in Cln3 that results in a hyperstabilized form of the protein (Cross 1988; Nash, Tokiwa et al. 1988). *WHI1-1/CLN3-1* mutants have a greatly shortened G1 but a similar doubling time to wild-type cells. Cln3 is an unstable, low abundance protein (Tyers, Tokiwa et al. 1992; Cross and Blake 1993), an activator of Cdc28 (Cross and Blake 1993), and a major controller of cell-cycle commitment.

1.2.5 Transcription regulation of Start

Transcription of over 100 genes at Start is mediated through the transcription factors SBF (Swi6/Swi4) and MBF (Swi6/Mbp1) (Nasmyth, Dirick et al. 1991; Dirick, Moll et al. 1992). SBF and MBF play a role in gene regulation themselves, and recruit other proteins, such as the Rpd3 HDAC complex(Wang, Garí et al. 2004) (Huang, Kaluarachchi et al. 2009; Takahata, Yu et al. 2009; Wang, Carey et al. 2009) and the repressor Whi5(Costanzo, Nishikawa et al. 2004; de Bruin, McDonald et al. 2004). Activation of SBF and MBF occurs independently by two proteins, the G1 cyclin Cln3 and the mysterious activator Bck2(Wijnen and Futcher 1999). Cln3 is a highly unstable protein(Tyers, Tokiwa et al. 1992; Cross and Blake 1993; Schneider, Patton et al. 1998) and Cln3 levels are regulated by transcription (Di Talia, Wang et al. 2009), translation (Gallego, Gari et al. 1997; Polymenis and Schmidt 1997; Danaie, Altmann et al. 1999), phosphorylation by Cdc28 (Tyers, Tokiwa et al. 1992) and phosphorylation by Protein Kinase A(PKA) (Michalewski, Kaczmarski et al. 1998). Cln3 levels are very tightly regulated, and *CLN3* is a dose-dependent activator of Start.

Cln3 promotes cell-cycle progression through Swi6, since a *GAL-CLN3 swi6* strain is unresponsive to *CLN3* induction (Wijnen, Landman et al. 2002).. Cln3/Cdc28, possibly via Swi6, is recruited to DNA (Wang, Carey et al. 2009) where the complex phosphorylates members of the SBF complex (Whi5, Stb1 and probably others) and converts the Swi4/Swi6/Rpd3/Sin3/Stb1/Whi5 complex from a repressor to a transcriptional activator. Activation of Cln3/Cdc28 results in inhibition and dissociation of the repressor Whi5, and the conversion of the repressor Stb1 into a transcriptional activator. A burst in transcription of genes involved in DNA synthesis and budding occurs. Among the target genes of SBF/MBF are the G1 cyclins Cln1 and Cln2, which activate SBF/MBF, and Nrm1, Clb5 and Clb6, which inactivate SBF/MBF. Thus, Cln3/Cdc28 generates a burst of transcription which is quickly amplified by a positive feedback loop, and drives cells through Start, and is turned off by a negative feedback loop, which keeps cells in S (Skotheim, Di Talia et al. 2008).

1.2.6 The Ras/cAMP/PKA pathway and control of carbohydrate metabolism

Budding yeast have several partially overlapping (Schmelzle, Beck et al.) pathways involved in modulation of cell growth in response to changes in nutrients, among them the TOR, PKA, Snf3/Rgt2/Yck and Snf1 pathways. The PKA/Ras/cAMP pathway is mostly involved in converting changes in carbon source into changes in cell-growth, via modulation of ribosome biogenesis, stress response and glycolysis. This pathway (Figure 1) consists of Gpr1, a G-Protein Coupled Receptor (GPCR) that interacts with the G-alpha subunit Gpa2. Gpa2, along with Ras (Ras1 & Ras2) activate the sole adenylate cyclase in budding yeast, Cyr1/Cdc35. The Ras-GEF Cdc25 also activates Cyr1. Both Cdc25 (Gross, Goldberg et al. 1992) and Gpr1 are regulated by glucose. Ras2 is activated by addition of glucose to cells, and this activation requires phosphorylation, but no further metabolism, of glucose, suggesting that internal glucose-phosphate may be able to activate the PKA pathway (Colombo, Ronchetti et al. 2004). Active Cyr1 catalyzes the circularization of ATP into cyclic AMP (cAMP, which activates Protein Kinase A (PKA, Tpk1,2 & 3) by binding to the PKA inhibitor Bcy1 and promoting dissociation of Bcy1 from PKA. Active PKA can promote cell-growth, glycolysis, cell-cycle progression (Matsumoto, Uno et al. 1983) and fermentation through the activation of transcription factors (e.g. Rap1 (Klein and Struhl 1994)) and metabolic enzymes (e.g. glycogen phosphorylase (Lin, Rath et al. 1996) and pyruvate kinase (Portela, Moreno et al. 2006)) (reviewed in (Santangelo 2006)).

The effect of PKA on carbohydrate metabolism is well established. Low levels of PKA activity activate carbohydrate synthesis, and high levels of PKA activity activate carbohydrate degradation. This regulation occurs two levels: a fast reaction involving phosphorylation of enzymes involved in synthesis and degradation, and a slower method of changing carbohydrate levels involving phosphorylation of transcription factors that regulate transcription of genes involved in carbohydrate metabolism. The different

methods by which PKA regulates carbohydrate levels has been excellently reviewed (François and Parrou 2001), and will be discussed here only briefly.

Glycogen phosphorylase (Gph1) catalyzes the release of glucose-1-P from linear chains of glycogen. Gph1 exists in two forms, an inactive unphosphorylated tetramer and an active phosphorylated dimer (Lin, Hwang et al. 1995; Lin, Hwang et al. 1997). Tetramerization is prevented by phosphorylation of the N-terminus of Gph1, as well as by complete removal of the N-terminal 42 amino acids. (Lin, Hwang et al. 1995; Lin, Hwang et al. 1997). PKA phosphorylates and activates Glycogen phosphorylase (Gph1) in vitro (Wingender-Drissen and Becker 1983), there is a conserved PKA consensus motif (RRL**T**) at amino acid 31 that is phosphorylated in vivo (Bodenmiller, Malmstrom et al. 2007) and Gph1 physically interacts with PKA (Tpk3) in vivo (Ho, Gruhler et al. 2002), but there is remains doubt that PKA phosphorylates Gph1 in vivo (Wingender-Drissen and Becker 1983; Lin, Hwang et al. 1995; Lin, Hwang et al. 1997).

Glycogen synthase (encoded by the paralogs Gsy1 and Gsy2) catalyzes the addition of UDP-glucose onto glycogen. Glycogen synthase exists in two forms: an activated dephosphorylated form, and an inactive phosphorylated form. Binding to glucose-6-phosphate (G6P) seems to stimulate dephosphorylation and activation, while the unbound form is preferentially phosphorylated. Therefore, the activity level of glycogen synthase is dependent not only on the balance between kinase and phosphotase, but also on the concentration of G6P, a precursor to UDP-glucose. Glycogen synthase is phosphorylated at three sites on its C-terminus, two of which are phosphorylated by Pho85 coupled to Pcl8 or Pcl10, and one by an unknown kinase. The phosphorylation state of GSY2 is dependent, in part, on PKA activity (Hardy, Huang et al. 1994). PKA may regulate glycogen synthase activity indirectly by targeting one of the kinases or phosphatases that directly act on glycogen synthase (Hardy and Roach 1993; Hardy, Huang et al. 1994; Huang, Wilson et al. 1997) or, perhaps, through the regulation of intracellular G6P levels (Huang, Wilson et al. 1997). In addition to post-translational regulation of *GSY2*, transcription of *GSY2* is strongly repressed by PKA phosphorylation of the transcription factors Msn2, Msn4 and Sok2 (Enjalbert, Parrou et al. 2004).

Trehalose is a disaccharide formed from UDP-glucose and glucose-6-phosphate. This reaction is catalyzed by four homologous subunits, encoded by TPS1, TPS2, TSL1 and TPS3. Trehalose synthase is not subject to phosphorylation, but is inhibited by inorganic phosphate and activated by fructose-6-phosphate (Londesborough and Vuorio 1993). Transcription of all four subunits is repressed by PKA activity through stress-responsive elements (STREs) in their promoters (Winderickx, de Winde et al. 1996).

Yeast has two trehalases, a cytoplasmic neutral trehalase (Nth1) and a vacuolar acid trehalase (Ath1). Nth1 appears to be responsible for all trehalase activity in growing yeast, as *nth1* mutants lack trehalase activity and fail to mobilize trehalose (Kopp, Muller et al. 1993). Nth1 exists as a homodimer and is activated by PKA phosphorylation of three sites in the N-terminal region (Wera, De Schrijver et al. 1999).

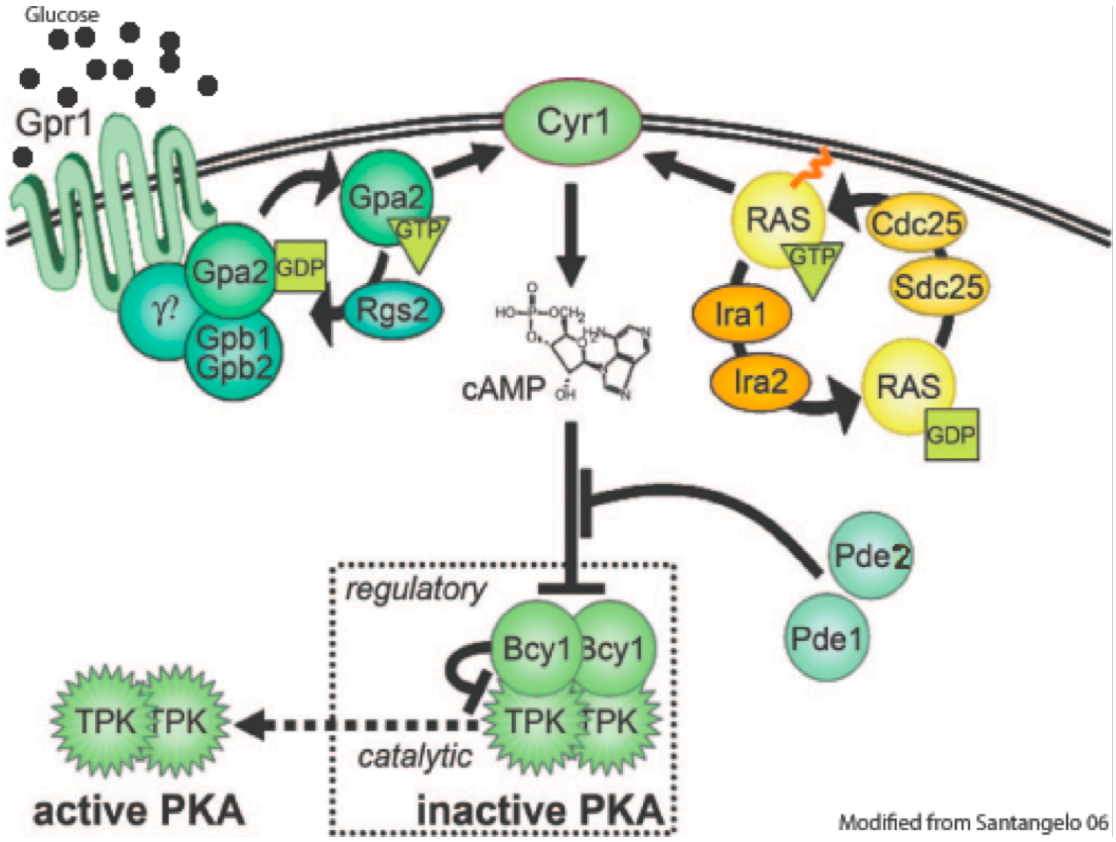

Figure 1. A Schematic of the RAS/cAMP/PKA pathway

An overview of the RAS/cAMP/PKA pathway. Glucose activates adenylate cyclase (Cyr1/Cdc35) via Gpa2. RAS activates Cyr1 independently and in parallel. Activation of the PKA pathway by either addition of glucose or by induction of a hyperactive allele of either RAS or Gpa2 results in an increase in cyclic AMP (cAMP) levels and activation of Protein Kinase A (PKA). Activation of PKA causes a direct (through phosphorylation of metabolic enzymes) and indirect (through phosphorylation of transcription factors) increase in translation, glycolysis, and respiration.

Chapter 2. cAMP and the finishing kick to Start

Yeast commit to the cell cycle in a size-dependent way: small cells do not pass through Start and commit to the cell cycle, while large cells do. Cells have a "Critical Size" to which they must grow in G1 phase before they can commit to cell cycle entry. During growth on ethanol, or in a glucose-limited chemostat, yeast undergo extensive changes in carbohydrate metabolism through the cell cycle. In early G1, carbon is stored as trehalose and glycogen up to 16% of dry cell weight. But in mid-G1, the stored trehalose and glycogen are broken down into glucose. This provides a burst of glucose and ATP over and above what can be supplied from the medium. It is at this time that cells express *CLN1* and *CLN2* mRNAs, and go through Start. Furthermore, it has been suggested (Muller, Exler et al. 2003) and I have confirmed (see below), that there is a spike in cAMP levels at about this same time in mid-G1; cAMP is a signaling molecule that shuts off glycogen synthesis, and promotes storage carbohydrate breakdown. It is possible that, for slowly growing cells, it is the storage of adequate trehalose and glycogen that constitutes the primary achievement of "Critical Size", and allows cells to pass Start and commit to the cell cycle. To test this idea, we have examined cells that cannot store carbohydrate, and found that indeed they have a larger critical size for Start than wild-type cells. An artificial spike of cAMP can in some circumstances decrease the critical size for Start, but only in cells capable of storing carbohydrate. The hypothesis that the amount of stored carbohydrates largely constitutes "Critical Size" does not apply to rapidly growing cells on abundant glucose (since they store no carbohydrates), but nevertheless it provides an answer to the size control problem for some kinds of cells.

2.1 Background & Introduction

Yeast growing slowly on a non-fermentable carbon source or in a glucose-limited chemostat have a low rate of protein synthesis (Schneider, Zhang et al. 2004) and a prolonged G1 during which they store large amounts of carbohydrate as glycogen and trehalose through early G1 (Paalman, Verwaal et al. 2003). Near the end of G1, prior to

Start, cells undergo a spike in cyclic AMP (cAMP) levels (Muller, Exler et al. 2003) and metabolize almost all of their stored carbohydrates (Silljé, ter Schure et al. 1997; Silljé, Paalman et al. 1999). In G1 during carbohydrate buildup, yeast generate ATP through respiration. At Start, around the same time that cells liquidate storage carbohydrates and exhibit a spike in cAMP, cells begin to generate most ATP through fermentation, and these formerly carbon-starved cells excrete ethanol and acetate into the media.

What is the reason for this straightforward but odd (formerly carbon-starved yeast now excrete carbon) sequence of events? The sudden, late G1-phase liquidation of stored carbohydrates (up to 16% of dry cell weight) allows slowly-growing cells a metabolic burst during which they can synthesize sufficient cyclin (which is unstable), and perhaps other limiting proteins. In addition, it allows the cells to synthesize DNA under glycolytic rather than respiratory conditions, possibly reducing the exposure of DNA to free radicals, and so possibly reducing DNA damage (Tu and McKnight 2007).

This metabolic burst, which we call "the finishing kick", suggests the possibility of an ingenious method for size control in slow-growth conditions. Cells might somehow monitor the level of stored carbohydrate as a measure of the cell's readiness to commit to the cell cycle. Cells could monitor storage carbohydrate levels directly, or they might monitor glycolytic flux, which would be reduced by buildup and increased by breakdown of carbohydrates. Breakdown of storage carbohydrates generates intracellular glucose (from trehalose) and glucose-1-phosphate (from glycogen), and addition of glucose to media can increase PKA activity and ribosome biogenesis (Wang, Pierce et al. 2004). The increase in ribosome biogenesis should lead to an increase in G1 cyclin (Cln) protein levels – larger cells produce more Cln protein (Schneider, Zhang et al. 2004) and ribosome levels are intimately related to size control and progression through Start (Jorgensen, Nishikawa et al. 2002; Bernstein, Bleichert et al. 2007). See Figure 8 A and B for a diagram of data supporting this hypothesis, and Figure 8 C for a cartoon version of this hypothesis.

This behavior, which gives otherwise slowly growing cells a burst in metabolism, provides cells with two things: a mechanism by which cells can synthesize enough cyclins to pass through Start, a mechanism for monitoring the cell's readiness to commit to the cell cycle – the level of stored carbohydrates. As the level of stored carbohydrates increase, the amount of carbohydrate being liquidated by glycogen phosphorylase (Gph1) or trehalase (Nth1) may increase in proportion to the amount of storage carbohydrate. Additionally, as the level of storage carbohydrates rise, the amount of glucose diverted into storage carbohydrates may decrease due to product inhibition. Combined, these two processes would result in increased glycolytic flux, which is associated with activation of adenylate cyclase and an increase in cAMP levels. High PKA activity will increase glycolytic flux, and further decrease deposition and increase liquidation of carbohydrates, thus creating a positive feedback look by which carbohydrates are degraded, cAMP levels rise, and ribosome biogenesis and metabolic flux both increase. It is likely that metabolic flux is a more accurate measure of the current extracellular environment than, for example, cellular volume or total cellular protein content. I and others (Grose, Smith et al. 2007) propose that cells monitor metabolic flux instead of the concentration of any particular metabolite. A high metabolic flux and high PKA activity result in a higher rate of protein synthesis, providing a mechanism for making enough Cln protein for cells to pass through Start.

This model, in which mobilized storage carbohydrates provide a burst of energy which the cell uses to increase Cln protein production and drive through Start is the "Finishing Kick" hypothesis (Futcher 2006). This model makes several predictions: that storage carbohydrate mutants should have cell size phenotypes, that cells growing in ethanol should be similar to glucose grown cells around Start and that the spike of cAMP in late G1 should help cells progress though Start.

2.2 Results

2.2.1 Slowly growing cells become rapidly growing cells around Start

Mobilization of large amounts of glycogen and trehalose and an increase in cAMP levels, as is seen around Start in carbon limited growth, might result in a burst of glycolysis, ribosome biogenesis, and glycolytic flux. I used microarrays to show that ethanol grown cells at Start look transcriptionally like glucose spiked or PKA pathway activated cells. Transcriptional changes and an increase in PKA activity suggest that slowly growing carbon-deprived cells briefly become rapidly growing carbon-rich cells around Start. I also observe an increase in growth rate during G1 in response to a spike of exogenous cAMP. I propose that an increase in biosynthetic capacity in response to an sudden burst of intracellular glucose turns slowly growing cells into rapidly growing cells and drives them through Start.

Slowly growing cells have a problem: they make less protein than rapidly growing cells, and are unable to accumulate high levels of the unstable G1 cyclins (Schneider, Patton et al. 1998; Honey, Schneider et al. 2001; Schneider, Zhang et al. 2004) to activate SBF and pass through Start. One way in which cells might switch from low to high Cln/CDK state is to increase the total amount of Cln protein they are able to produce by increasing the number of ribosomes. Both liquidation of stored carbohydrates and a spike in cAMP levels, independently or together, should produce a switch from slow growth to rapid growth. This switch can be identified in two ways: as a transcriptional response, and as increase in the rate of growth.

A spike in cAMP should result in transcription of ribosomal genes (via Rap1 (Klein and Struhl 1994) and Fhl1 (Martin, Soulard et al. 2004)). When given a brief pulse of glucose, ethanol grown cells ferment the glucose, releasing ethanol and acetate into the media. They then express genes involved in the metabolization of ethanol and acetate (van den Berg, de Jong-Gubbels et al. 1998). Ethanol grown cells exhibit a similar pattern of gene expression (Figure 2). Around Start, where there is a burst of PKA activity and perhaps a burst of glucose due to liquidation of storage carbohydrates, yeast turn on

genes involved in ribosome biogenesis. Expression of ribosomal genes peaks around Start and may be slightly repressed in G2/M (Figure 2).. In G2/M a new set of genes, those involved in respiration and generation of acetyl-coenzyme A from the byproducts of fermentation (ethanol and acetate), are turned on (Figure 2). This pattern of gene expression is not seen in glucose grown cells (Figure 3 and data not shown).

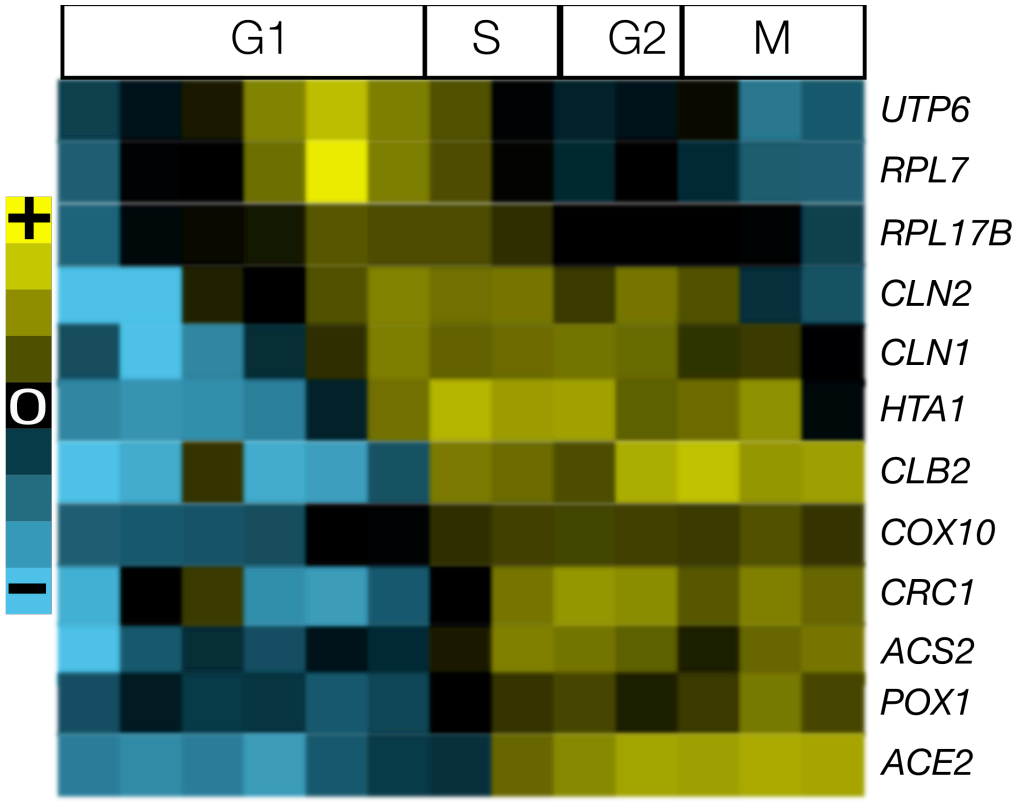

Figure 2. Transcription of ribosome biogenesis and metabolic genes during the cell-cycle

Small unbudded G1 daughters growing in YPE at 25°C were obtained by centrifugal elutriation. Cells were grown at 25°C and samples were taken every 30min for microarrays. Transcription of cyclins (*CLN1*, *CLN2*, *CLB2*), histones (*HTA1*) and the transcription factor *ACE2* is cell-cycle regulated in all growth conditions (Spellman, Sherlock et al. 1998). In this ethanol elutriation genes involved in ribosome biogenesis (*UTP6*, *RPL7*, *RPL17B*) are cell cycle regulated and peak around Start. Genes involved in respiration (*COX10*) and the generation of acetyl-coenzyme A from acetate (*ACS2*) and beta-oxidation (*POX1* and *CRC1*) are expressed in G2/M. Cell-cycle regulated transcription of these genes does not occur in glucose grown cells (data not shown).

In order to investigate the transcriptional response around Start on a broader scale I examined changes in gene expression in cell-cycle synchronized cells for genes that are known to be part of the cell's response to glucose or PKA pathway activation. Wang et al. (Wang, Pierce et al. 2004) recently defined eight classes of genes based on their transcriptional response to glucose addition in wild-type and *tpk-w* strains, and in response to hyperactivation of the PKA pathway (See Table 1 for class definitions). If glucose is released (via the degradation of storage carbohydrates) just before Start, then glucose inducible genes should be turned on around Start, and this should only occur in cells that store carbohydrate. By looking at the expression of glucose and PKA responsive genes as an indirect assay of the glucose release and PKA activity we can use microarrays to obtain an indirect readout of the cell's metabolic state.

Table 1. Classes of genes in response to glucose and/or PKA

Class	# Genes	WT +Glu	PKA activation	*tpk-w* +Glu	Description
I	855	I	I	I	Induced+/- PKA
II	161	I	I	--	Induced. Requires PKA
III	128	I	--	I	Glucose Induced, PKA Independent.
IV	154	I	I	R	Induced by glucose and PKA, requires PKA.
V	579	R	R	R	Repressed +/- PKA
VI	314	R	R	--	Repressed. Requires PKA
VII	278	R	R	I	Repressed by glucose. Requires PKA.
VIII	804	--	--	R	Repressed by glucose only in the absence of PKA signaling.

Wang et al. identified eight classes of genes based on their transcriptional response to PKA hyperactivation and glucose addition. Four of these gene classes show strong cell-cycle regulated transcription in ethanol grown cells. In the table I is induced, R repressed, and -- is for classes with no significant change in the listed growth condition and genotype.

I found that these four classes of genes have a distinct cell-cycle expression profile in ethanol grown cells (Figure 3). Around Start there is transcriptional activation of Class I genes and repression of Class V genes, as would be expected due to liquidation of storage carbohydrates and a spike in cAMP levels. Following Start, expression of these two

classes becomes indistinguishable from the genome as a whole during S and G2, but then, in mitosis the glucose repressed genes (Class V) are induced and the glucose induced genes (Class I) are repressed. Here the cell may be reverting to its slow-growth phase. Then, in late G1 the glucose induced genes (Class I) turn on again. This pattern is highly visible in YPE (2% ethanol) grown cells in an elutriation (Figure 3 A & B). There is no apparent cell-cycle regulated transcription of any PKA or glucose responsive genes in an alpha-factor synchronized cells grown on glucose (Figure 3 C & D). The cell-cycle transcriptional regulation of PKA and glucose responsive genes is specific to ethanol grown cells, consistent with the hypothesis that it is related to the breakdown of carbohydrates around Start.

In the elutriation each peak of differential expression (at Start and in G2/M) is represented by a series of at least three timepoints in which all four classes of genes are expressed at highly different levels from the genome as whole (p-value < e^{-10}). The only region of the glucose cell-cycle in which there is a multi-timepoint peak is upon release from alpha-factor. This is likely an artifact of the alpha factor; there is no significant change in gene expression in the second cell-cycle, nor following release from a *cdc28-13* block and release (Figure 3 and data not shown).

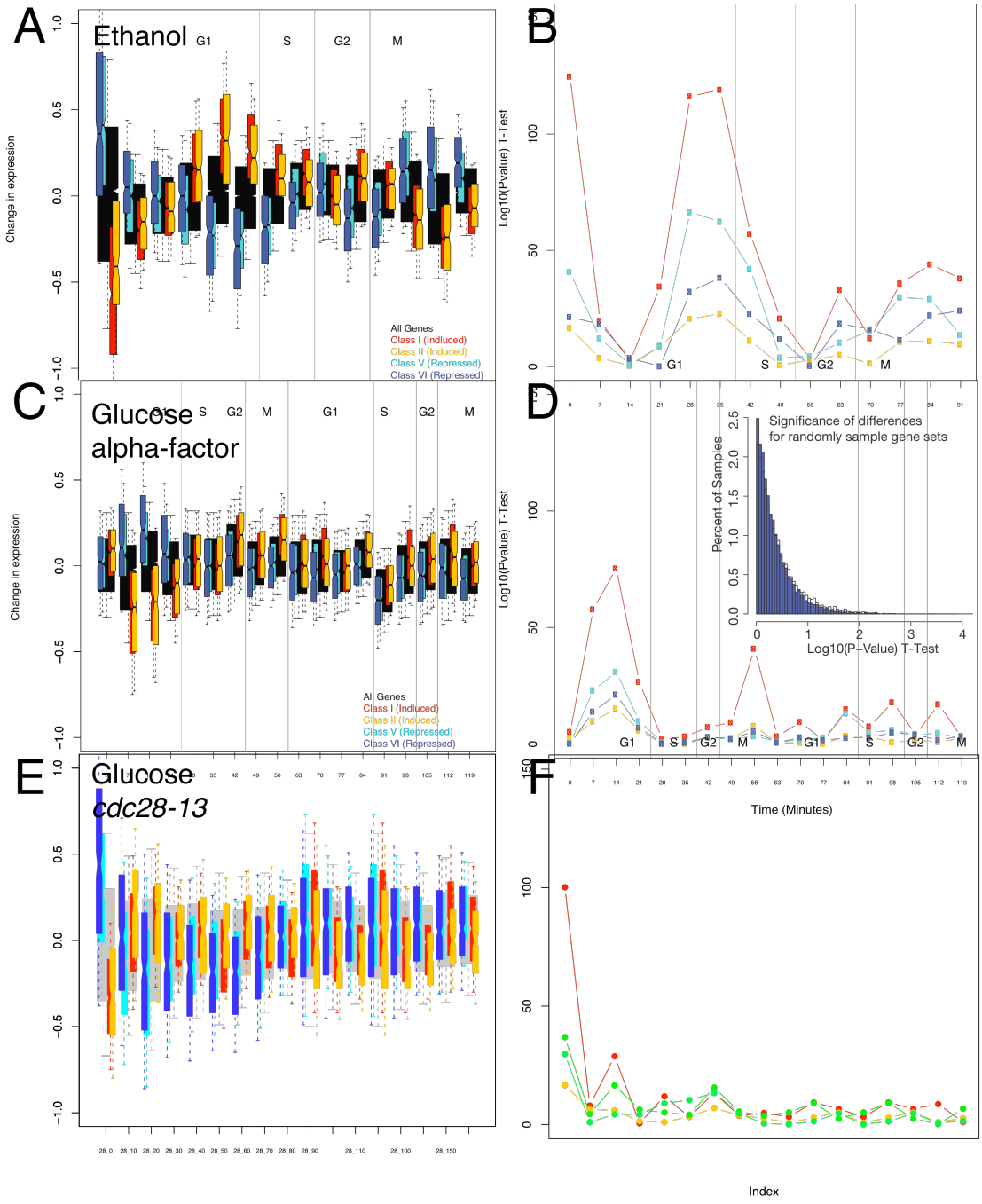

Figure 3. PKA and glucose responsive genes are cell-cycle regulated only in ethanol

Graphs of the range of expression levels of PKA and glucose responsive genes through three different cell-cycle synchronization methods. Cells were grown in ethanol and synchronized by elutriation (A) or grown in glucose and synchronized by either alpha-factor (C) or *cdc28-13* (E) block and release. In (A,C,E) each rectangle represents the range of expression values for the specific class of genes at the given time point. The notches show the median expression level for each set of genes, and the hinges show first and third quartile. Dashed lines (whiskers) show the interquartile range. Black or grey bars are the complete genome (all transcripts). Class I genes (glucose and PKA pathway induced) are shown in red. Class II genes (Glucose and PKA induced, PKA dependent) are shown in orange. Class V genes (Glucose and PKA repressed) are shown in light blue. Class VI genes (Glucose and PKA repressed, PKA dependent) are shown in dark blue. A t-test was used to determine which sets of genes at which timepoints are expressed significantly different from the genome as a whole (B,D,F). The inset in (D) shows a histogram of Log10(P-Values) from 1000 iterations for 850(blue) or 150(white) randomly selected genes, showing the range of expected p-values from randomized data.

Activation of the PKA pathway is associated with rapidly growing cells (Klein and Struhl 1994). To see if a spike in cAMP results in faster growth, I grew *pde2* yeast (which, unlike wild-type cells, are responsive to extracellular cAMP) in YPE and obtained small unbudded G1 cells via elutriation. I then spiked cells with either 2mM cAMP or AMP for 15 minutes and measured cell volume over time for each culture. Cells spiked with cAMP grew faster than those spiked with AMP (Figure 4). The spike in cAMP increases the growth rate even in *pde2* cells, which have a high basal cAMP. It is likely that the intracellular spike in cAMP around Start observed in synchronized cultures increases the growth rate in wild-type cells as well.

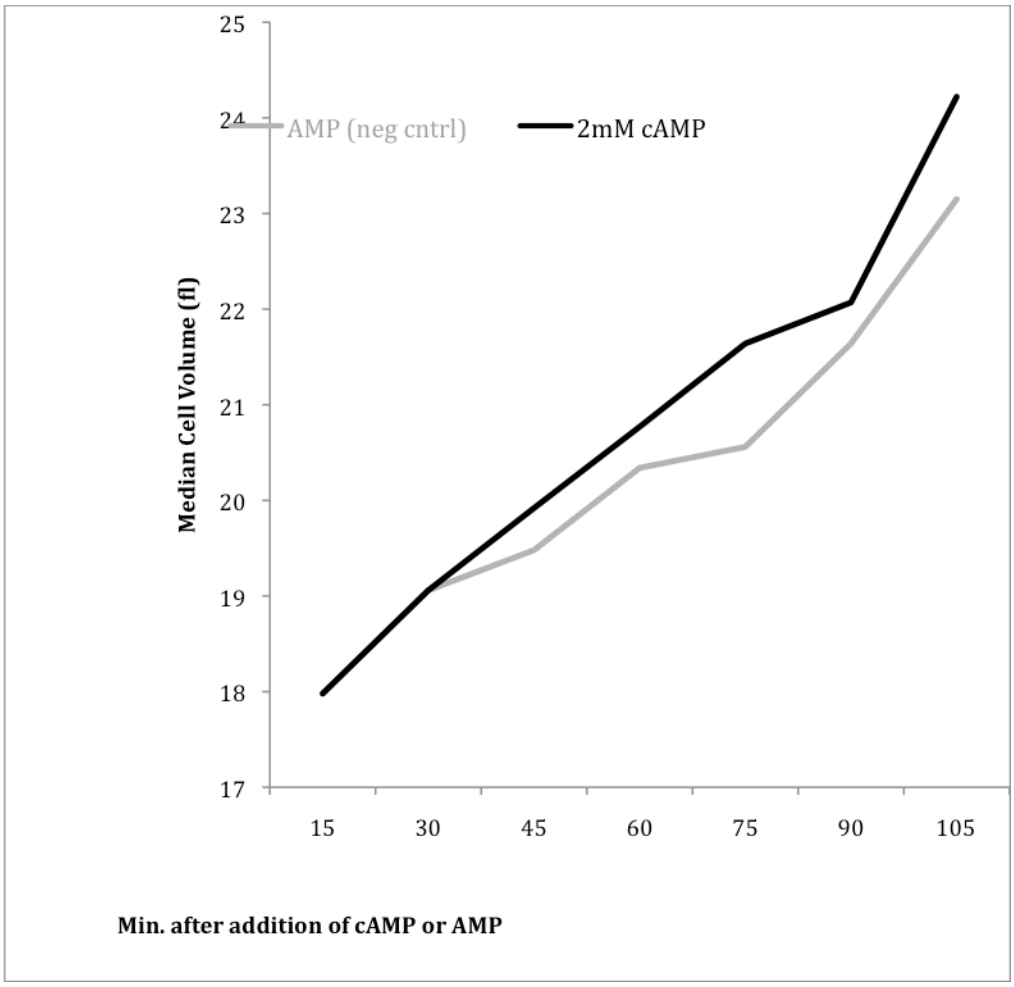

Figure 4. Addition of extracellular cAMP results in an increase in growth rate.

Small unbudded G1 daughter *pde2* cells of approximately 16fl were obtained by centrifugal elutriation and split into two fractions. Cells were spiked with either 2mM cAMP or AMP for 15 minutes, washed, and resuspended in YPE. Cell volumes were measured approximately every 15 minutes and the median cell volume of the population was recorded. The cells in the culture to which cAMP was added increased in volume more quickly than cells in the culture to which AMP was added.

2.2.2 Identification of genes that are targets of both Cyclin/Cdc28 and PKA

Commitment to the mitotic cycle, Start, occurs when cells switch from a low Cln/CDK state to a high Cln/CDK state. Around the same time storage carbohydrates are degraded, there is a spike in cAMP levels, and cells switch from respiration to fermentation. In addition to the spike at Start, there is a rise in cAMP levels around mitosis and the PKA may participate in the DNA damage checkpoint (Searle and Sanchez 2004). Regulation of cell-cycle controlling genes by PKA, and regulation of metabolic regulatory genes by CDK would be a mechanism by which the cell could co-regulate the growth and division cycles. A molecular link between PKA and G1 cyclin regulation and cell-size is well established (Hubler, Bradshaw-Rouse et al. 1993; Baroni, Monti et al. 1994; Mitsuzawa 1994; Tokiwa, Tyers et al. 1994; Hall, Markwardt et al. 1998), yet few people have looked into coregulation of genes that are co-regulated by CDK and PKA (Futcher 2009; Kurat, Wolinski et al. 2009). I performed a computational screen to look for genes that might be coregulated by CDK and PKA. The screen has two intentions: to examine the potential overlap in targets between the two kinases, and to identify a few potential candidates for further study (eg: by mutating the predicted phosphorylation sites and looking for a phenotype). I found that many genes involved in regulation of both cell-cycle control and carbon metabolism have both CDK and PKA sites, many of which have been shown to be phosphorylated in vivo using mass-spec. In addition, many of these proteins that are predicted targets of both CDK and PKA have been shown to physically interact with both kinases. I suggest that there is a large amount of cross talk between the two kinases, and that this may aid in maintaining a strong link between the cell's metabolic state and the cell cycle. The screen has also provided us with some very interesting leads for making phosphorylation-site mutants.

Important molecular links between PKA and CDK may be conserved among the *Ascomycota*. Wapinksi et al (Wapinski, Pfeffer et al. 2007) generated 11,103 groups of orthologous genes containing 102,044 ORFs for seventeen *Ascomycota* fungi. To look for possible targets of both PKA and CDK I looked for orthogroups that are enriched for

both PKA (R[RK]X[ST]) (Budovskaya, Stephan et al. 2005) or CDK ([ST]P) sites. I did not look for conservation of the location of the phosphorylation site, as precise conservation of the location on phosphorylation sites is often unimportant (Chang, Begum et al. 2007; Holt, Tuch et al. 2009). The list of possible PKA and CDK targets contains many genes known to be involved in cell-cycle control, and many genes known to be involved in metabolism (Table 2). The list contains many major cell-cycle regulatory genes (e.g.: Whi5, MCM, Pds1) that may be regulated by PKA and several major metabolic genes (e.g.: Nth1, Gph1, Bcy1) that may be regulated by CDK.

For each orthogroup I calculated a kinase site enrichment score (see Equation 1) to determine if the genes in the orthogroup are enriched for potential CDK and PKA sites. I counted the number of phosphorylation site motifs in each orthogroup ($NS_{orthogroup}$). I also calculated the number of amino acids in the orthogroup ($AA_{orthogroup}$) and the frequency of the phosphorylation site motif in the set of all fungal proteomes (SF_{fungi}). Site enrichment was calculated based on the frequency of the motif in all seventeen proteomes and length of the proteins in the orthogroup; this provides a protein length independent estimate for the number of potential kinase targets in each orthogroup.

$$Enrichment = \frac{NS_{orthogroup}}{AA_{orthogroup} * SF_{fungi}} \quad (1)$$

Both CDK and PKA motifs occur with high frequency in the proteome; many of these sites may not be phosphorylated by the relevant kinase. To estimate how many of the genes whose orthogroups are enriched for PKA or CDK sites are real substrates I asked which proteins been found by proteome-wide in vivo or in vitro studies to physically interact with both PKA and CDK. Several groups have done various types of proteome wide physical interaction screens as well as in vitro kinase target screens (Ptacek, Devgan et al. 2005) (Ubersax, Woodbury et al. 2003; Holt, Tuch et al. 2009). I find that biochemically confirmed targets of both CDK and PKA have a high enrichment score (see Figure 5), strongly suggesting that these genes might be regulated by CDK and PKA phosphorylation.

Table 2. Genes enriched for CDK and PKA sites that are biochemical vivo or in vitro kinase targets

Gene	PKA Enrich	CDK Enrich	Product
WHI5	3.68	12.11	44.60
LRS4	3.00	8.00	24.00
PDS1	3.33	4.67	15.56
STB3	2.58	2.58	6.68
MPS2	1.89	3.51	6.65
VHS2	2.96	2.11	6.25
HAS1	1.02	5.20	5.31
SAS10	1.98	2.17	4.30
PAH1	0.97	3.88	3.76
CWC25	1.82	2.00	3.64
BUD6	1.52	1.86	2.83
MCM3	0.74	3.40	2.51
PXL1	1.23	1.96	2.41
MCM4	0.86	2.78	2.40
ALY1	1.23	1.86	2.29
GPH1	1.17	1.90	2.22
PRR1	0.98	2.25	2.21
SSD1	1.03	1.93	1.99
KEL1	0.79	2.03	1.60
UBP9	1.69	0.90	1.52
RNH70	1.49	0.88	1.31
BCY1	3.03	0.39	1.19
NTH1	1.60	0.65	1.04
UBP10	1.28	0.73	0.94
SPT16	0.38	1.36	0.52
PCK1	0.23	1.03	0.24

This table contains all genes whose orthogroups are enriched for either CDK or PKA sites, and for which there is biochemical evidence of in vitro or in vivo phosphorylation by both CDK and PKA.

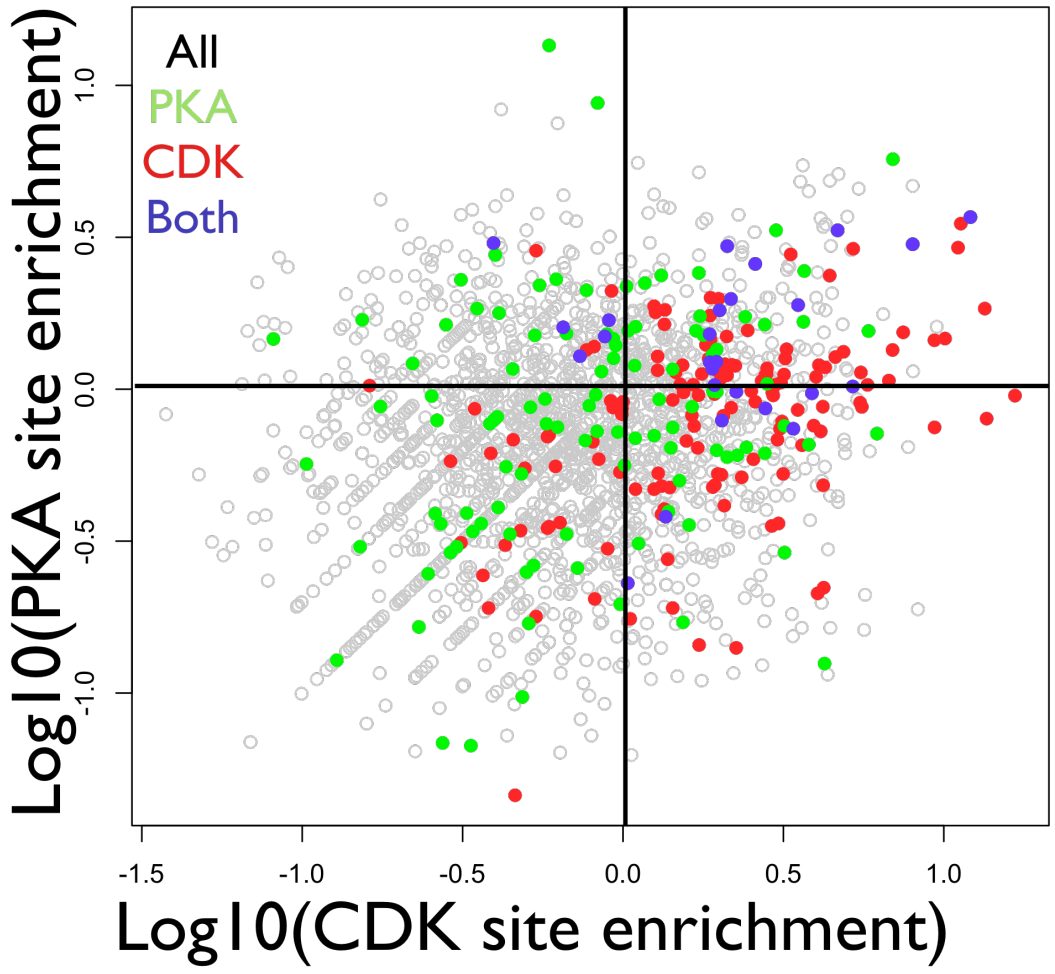

Figure 5. Genes that are targets of both PKA and CDK are members of orthogroups that are enriched for both PKA and CDK motifs.

Enrichment of PKA and CDK motifs in groups of orthologous genes (grey). Genes that are in vitro or in vivo targets of CDK (red). Genes that are in vitro targets of PKA (green). Genes found as biochemical targets of both PKA and CDK (blue). The X and Y axes are the enrichment for CDK and PKA sites respectively in the computational screen. Genes with scores above 0 have orthogroups enriched for the kinase motif. True CDK targets tend to be enriched for CDK sites (red dots are mostly to the right of 0) but this is not the case for true PKA targets (green dots are uniformly distributed in Y). Most genes that have been biochemically identified as targets of PKA and CDK are in the upper right quadrant. These genes belong to orthogroups that are enriched for both PKA and CDK sites.

2.2.3 Changes in storage carbohydrate levels change the timing of Start

The "Finishing Kick" model, in which liquidation of storage carbohydrates produces a glycolytic and energetic burst that drives cells through Start, predicts that cells lacking storage carbohydrates should have a larger critical size. I obtained a *gsy1 gsy2 tps1* strain, which is unable to store carbohydrates since both glycogen and trehalose synthesis are disrupted (Guillou, Plourdeowobi et al. 2004). I grew both WT and carbohydrate null strains in YPE, collected small unbudded G1 daughters by centrifugal elutriation, and measured cell volume and budding while cells grew. If carbohydrate liquidation aids cells in progression through Start, then we expect the carbohydrate null strain to have a larger critical size, and that is indeed what I found (Figure 7 A). The larger cell size in the carbohydrate null suggests that liquidation of storage carbohydrates aids in timely progression through Start.

Around Start yeast exhibit a spike in cAMP and exhibit a transcriptional response similar to yeast given an extracellular glucose spike. The spike in cAMP levels (Muller, Exler et al. 2003) might be the cause, or it might be the effect, of liquidation of storage carbohydrates. In support of the former, PKA activates carbohydrate breakdown and inhibits synthesis. In support of the latter, addition of glucose (similar to what would be experienced during liquidation of carbohydrates) produces a spike in cAMP. Both may be true; there may be a positive feedback loop in which slight liquidation of carbohydrates leads to increased glycolytic flux (from freed G6P), which leads to an increase in cAMP levels, causing higher PKA activity and increased carbohydrate degradation (see Figure 8 A).

To see if a spike in cAMP can promote Start, possibly via induced liquidation of storage carbohydrates, I used centrifugal elutriation to collect small unbudded G1 *pde2* daughters. I spiked a synchronous fraction of cells for 15 minutes with either 2mM

cAMP or 2mM AMP. Cells were then washed and resuspended in preconditioned pre-warmed YPE. Cells spiked with cAMP budded at a smaller size relative to control cells spiked with AMP (Figure 7 C). Since an exogenous spike in cAMP can promote Start, this suggests that the spike in cAMP that cells naturally exhibit might promote Start as well.

There is some evidence that in cells unable to metabolize sucrose (*suc2*/invertase null), addition of sucrose causes a spike in cAMP (Lemaire, Van de Velde et al. 2004). To see if addition of sucrose to *suc2* cells might promote Start, possibly through a spike in cAMP, I collected small unbudded G1 *suc2* daughters in a similar experiment as above. Addition of sucrose resulted in cells going through Start at a smaller size, similarly to exogenous cAMP addition to *pde2* cells (data not shown).

A model in which the spike in cAMP promotes Start via liquidation of storage carbohydrates and the subsequent increase in available glucose phosphate predicts that, in the absence of storage carbohydrates, the spike in cAMP will be unable to promote Start. A *gsy1 gsy2 tps1 pde2* strain lacking the cAMP phosphodiesterase as well as all carbohydrate synthesis genes was grown in YPE and small unbudded G1 cells were obtained by elutriation and treated identically as above. Consistent with a model in which the cAMP spike promotes Start via liquidation of carbohydrates, the spike in cAMP was unable to promote Start in the absence of storage carbohydrates (Figure 7 D).

If cells wait to reach a critical level of storage carbohydrates, at which point they undergo a cAMP spike and pass through Start, then changing the rate of deposition of storage carbohydrates should alter the timing of Start. Storage carbohydrate levels can be doubled by over-expression of a hyperactive form of *GSY2* (*GSY2 Δ 643*) (Pederson, Cheng et al. 2000; Pederson, Wilson et al. 2004; Torija, Novo et al. 2005), or by over-expression of wild-type glycogen synthase. I expressed either wild-type or hyperactive (*GSY2 Δ 643*) glycogen synthase in otherwise isogenic strains grown in SC-Trp raffinose medium and measured cell volumes in asynchronous cultures. Median cell volumes were significantly smaller in cells expressing the hyperactive form (Figure 6 A). In a similar

experiment I transformed cells with a high-copy plasmid containing either a genomic fragment with full-length *GSY2* or a similarly sized fragment whose 5' end was in the middle of *GSY2* but did not encode an active protein (Jones, Stalker et al. 2008). Introduction of the fragment containing full length *GSY2* makes cells smaller than the fragment lacking full length *GSY2* (Figure 6 B). Excess glycogen synthesis makes cells smaller, possibly because cells somehow monitor carbohydrate levels.

If yeast monitor carbohydrate levels to control progression through Start, but this monitoring requires liquidation of carbohydrates, then, in addition to excess carbohydrate synthesis making cells smaller, and lack of storage carbohydrate making cells larger, the inability to liquidate carbohydrates should also make cells larger. To test this, I grew otherwise isogenic wild-type and glycogen phosphorylase null mutants (*gph1*) in YPE (2% ethanol) and in YPD (2% glucose). In YPE the *gph1* strains have a larger median cell volume than do wild-type cells (23.6, 22.3 and 21.1fl for three independent colonies of *gph1* yeast compared to 18.2 and 15.9 for two independent colonies of wild-type cells). On YPD there is no difference in sizes (data not shown), as would be expected for a growth condition in which carbohydrates probably play no role. These data suggest that something about the influence of carbohydrates on cell size requires mobilization of the carbohydrates.

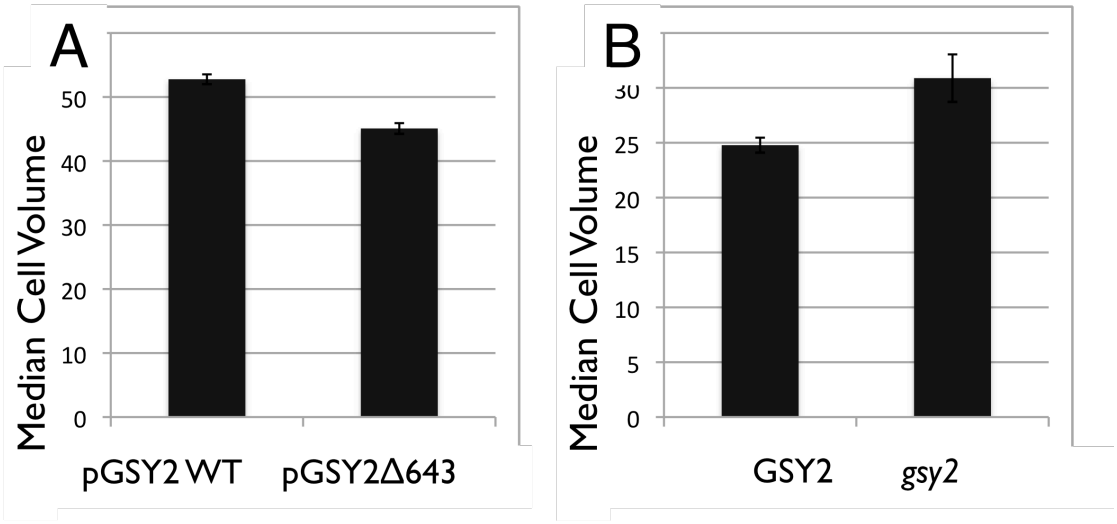

Figure 6. Cells with increased glycogen synthase are smaller

Wild-type cells containing a plasmid expressing either wild-type or a non-regulatable isoform of glycogen synthase (GSY2-Δ643) were grown in SC-Trp media with raffinose as the carbon source (A). Cells with a 2uM plasmid with a genomic fragment with wild-type GSY2, or a control plasmid that carries a genomic fragment containing only the 3' half of *gsy2* were grown in SC-Leu media with raffinose as the carbon source (B). At least five separate transformants for each plasmid were picked for each genotype for asynchronous culture size analysis.

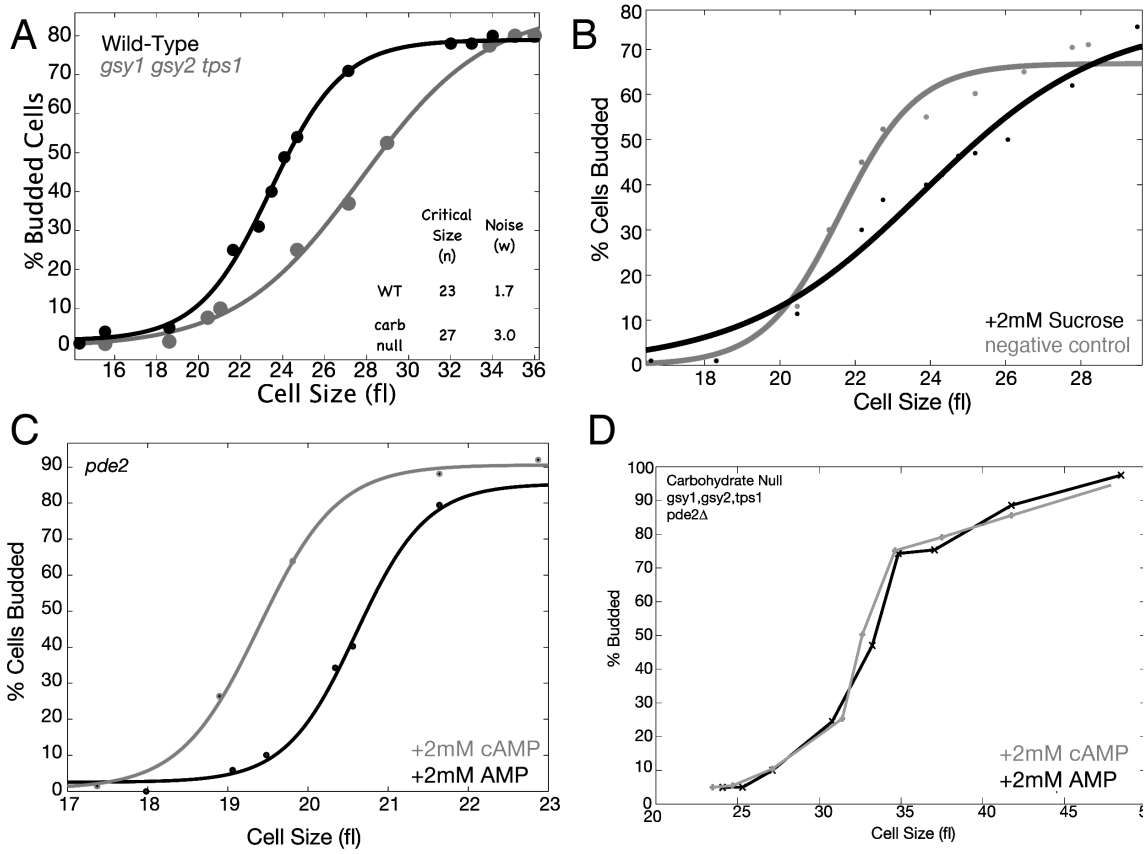

Figure 7. Effects of carbohydrate mutations and cAMP spikes on critical size

Small unbudded G1 cells were obtained by centrifugal elutriation. Isogenic carbohydrate null (*gsy1 gsy2 tps1*) cells and wild-type cells were elutriated and grown in YPE(A). *pde2* (C) or (*gsy1 gsy2 tps1 pde2*) cells (D) were grown in YPE, elutriated, and the fraction was split in two. Cells were spiked with either 2mM cAMP or AMP for 15 minutes, and grown in YPE. *suc2* cells were elutriated in YPE, split into two fractions, and spiked with either 2mM sucrose (B) or water as a negative control.

2.2.3.1 A spike of cAMP can promote start and speed up growth

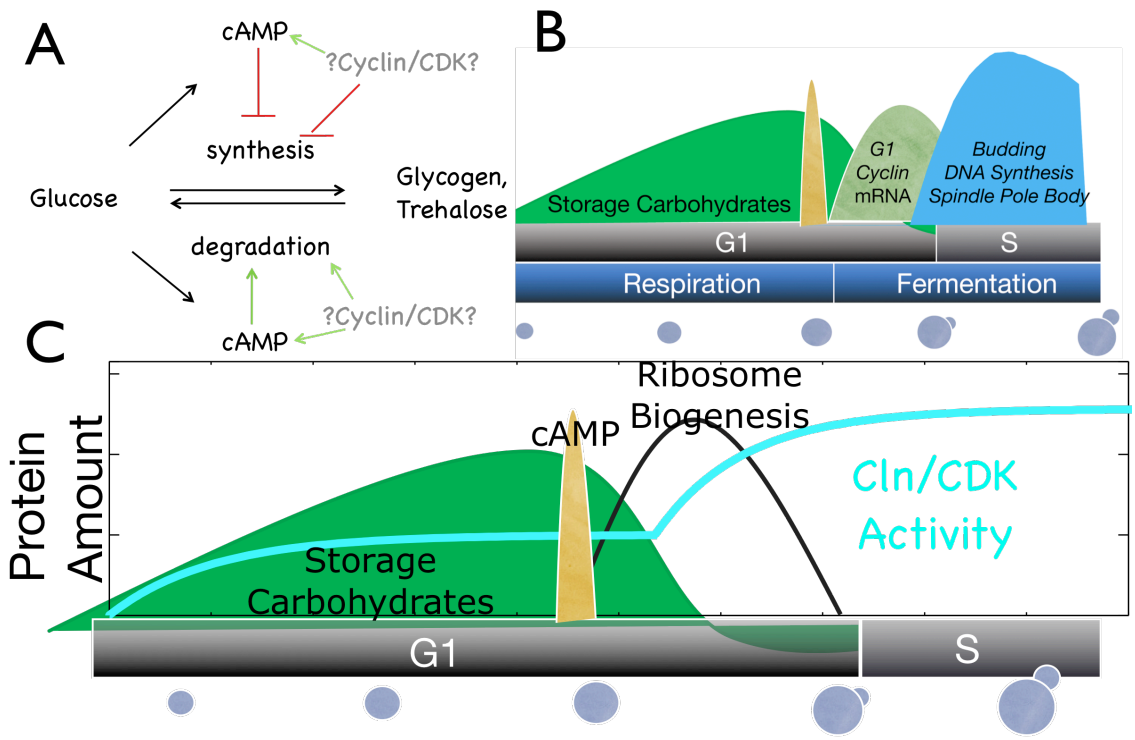

Figure 8. Cartoons for metabolism and cell-cycle progression

PKA activity promotes carbohydrate degradation and inhibits synthesis (A). (B) shows the known carbohydrate, cAMP, and transcriptional dynamics around Start. The placement of the cAMP spike relative to carbohydrate degradation is not know – the spike may precede, follow, or overlap with, carbohydrate liquidation. The increase in ribosome biogenesis around Start may help drive cells through Start by increasing the accumulation of unstable Cln protein (C).

2.3 Discussion

Yeast growing on ethanol build up storage carbohydrates during G1, and break them down around Start. Concomitant with a drop in storage carbohydrates, cells experience a large spike in cAMP levels. cAMP activates the cAMP dependent protein kinase (PKA) which, via phosphorylation of multiple proteins, promotes glycolysis, degradation of storage carbohydrates and protein synthesis. The 'Finishing Kick' model suggests that this energetic burst may help cells drive through Start by increasing Cln protein levels

above some critical threshold. I have provided several pieces of evidence that move this model forward.

Carbohydrate levels and the spike in cAMP influence critical size and cell-cycle progression. Lack of carbohydrate synthesis or lack of carbohydrate mobilization makes cells bigger; excess carbohydrate synthesis makes cells smaller. This suggests a mechanism by which cells might somehow measure their carbohydrate levels. This monitoring process requires carbohydrate degradation as well as synthesis.

Taken all together, I have shown (1) cells lacking storage carbohydrates have a larger critical size (2) cells with increased glycogen synthase are smaller, and cells unable to degrade glycogen are larger (3) a spike in cAMP can promote Start, but only in the presence of storage carbohydrates. These data suggest that cells may be monitoring storage carbohydrate levels in order to decide when to commit to cell-cycle progression. Accumulation of enough stored intracellular carbon would be a signal that the cell is energetically ready to progress through Start. As carbohydrate levels increase, the back reaction (from glycogen/trehalose -> glucose) due to basal phosphorylase/trehalse activity should increase with the absolute amount of carbohydrates in the cell. This would create an increase in glycolytic flux, which can cause an increase in cAMP levels. Glycogen phosphorylase and neutral trehalase are both activated by PKA, so an increase in PKA activity will lead to more carbohydrate degradation, creating a positive feedback loop in which once a critical level of carbohydrates is reached, carbohydrate stores are all degraded in one large energetic burst.

In addition, as cells get larger in G1, they make more Cln protein (Schneider, Zhang et al. 2004). Cln/CDK levels may also play a role in this liquidation and glycolytic burst as Bcy1, Gph1 and Nth1 may all be Cyclin/CDK targets.

I propose a model for size control in ethanol grown cells in which, as cells become larger, they exhibit more glycolytic flux (higher PKA activity) and higher Cln/CDK activity. Eventually a size is reached in which ever-rising Cln/CDK and PKA mediated

inhibition of carbohydrate synthesis reaches a critical point. There is massive liquidation of storage carbohydrates, creating an intracellular burst in glucose and in cAMP. This promotes not only more carbohydrate liquidation, but also ribosome biogenesis. Increased ribosomes lead to an increase in Cln protein production above a critical threshold, and passage through Start.

2.4 Materials and methods

2.4.1 Computational Screen

Orthogroups (Wapinski, Pfeffer et al. 2007) and fungal proteomes were downloaded from (http://www.broadinstitute.org/regev/orthogroups/). Proteomes were searched for PKA (R[RK]X[ST]) or CDK ([ST]P) motifs using a custom Perl script. Kinase targets for PKA and CDK were obtained from the supplementary data for each paper (Ptacek, Devgan et al. 2005) (Ubersax, Woodbury et al. 2003; Holt, Tuch et al. 2009). Data was uploaded into a custom MySQL database and further analyzed using R and Perl.

2.4.2 Transcriptome analysis

Microarray time course data (Spellman, Sherlock et al. 1998) was obtained from (http://genome-www.stanford.edu/cellcycle/). Glucose and PKA regulated genes (Wang, Pierce et al. 2004) were obtained from the supplementary data. Data and gene lists were uploaded into a custom MySQL database and analyzed with custom R scripts. Significant up or down regulation of gene classes was calculated using a T-test to compare the expression of the entire genome with the expression of each class at each time point. Significance of difference (Figure 3 D inset) was calculated by randomly selecting groups of either 850 (blue) or 150 (white) genes and comparing the expression level of the randomly selected group to the rest of the genome.

2.4.3 Cell growth and size measurement

Strain construction and growth conditions. Yeast strains were grown and sporulated, and strains constructed according to (Amberg, Burke et al.). See Table I (to be completed) for a list of strains used. Cells were grown in YP (1% yeast extract, 2% peptone, .2mM adenine) or SC (0.17% Yeast Nitrogen Base without amino acids (YNB),

0.5% ammonium sulfate, and all amino acids required for auxotrophic strains). For experiments in which only a single carbon source was used, or where there was one carbon source common to all growth conditions, media was prepared containing 2% w/v of the common carbon source. For experiments with varied carbon sources, media was prepared without carbon, and carbon sources were prepared separately as 20% (10x) stocks. Media used in this study are: YP + Ethanol (YPE), YP + Raffinose (YPRaf), YP + Galactose (YPGal), YP + Raffinose + Galactose (YPRG), YP + Glycerol (YPGly), YP + Dextrose (YPD) and YP + Sucrose (YPSuc). SC versions (SCE, SCRaf, SCGal, SCRG, SCGly, SC[D] and SCSuc) and of all these media were used as well. Sucrose and raffinose stocks were prepared by filter sterilization; all other carbon sources were autoclaved. Yeast cells were grown at 30°C in flasks or tubes less than 1/3 full with media unless otherwise stated. For experiments performed on non-fermentable (glycerol and ethanol) or poorly fermentable carbon sources (raffinose), cells cultures for experiments were started from cultures previously grown a minimum of three days in the relevant carbon source to acclimate the cells to respiration. Many strains were grown to saturation on glycerol or ethanol before being frozen so that stocks revived efficiently on glycerol/ethanol plates. Strains were generated using standard methods (Amberg, Burke et al.): either by crosses and tetrad dissection or by transformation and homologous recombination of PCR products or plasmids.

Cell-cycle synchronization of cells. Elutriations were performed as described (Futcher). Briefly, cells were grown for at least three days in Synthetic Complete (SC) medium in the relevant carbon source with nightly dilutions. Small unbudded G1 cells were isolated by centrifugal elutriation and grown in the same medium in which they were growing before elutriation. Cultures were incubated at 30°C on a shaker and samples were collected and placed on ice every seven to twenty minutes depending on the experiment. Size distributions were obtained on a Z2 Coulter Counter and budding indexes were determined by manually counting cells. Bud counts were performed either 'blind' or in random order to avoid experimenter bias. Cell volumes were extracted from the Z2 data files using a custom Perl script and cell volumes and growth rates were measured using R and Excel. Curves in Figure 7 were generated by fitting budding and

size data to a sigmoidal equation (Equation 2) (Ledvij 2003) using MatLab. In Equation 2 A_b and A_t are the minimum and maximum fractions of budded cells during the elutriation (in a perfect elutriation, they would range from 0 – 100). Y is the fraction of budded cells and x is cell volume. This equation can be fit to elutriation data to produce values for n (the size at the midpoint between A_b and A_t – a measure of critical size) and w (the width of the sigmoidal part of the curve – a indicator of cell-to-cell variability in both the elutriation and size control).

$$Y = A_b + \frac{A_t - A_b}{1 + e^{-\frac{x-n}{w}}} \tag{2}$$

Asynchronous Cell Size. Cells were grown overnight in the relevant media, resuspended in fresh media and grown for at least three generations so that cell densities were between 1 and $2*10^7$ cells/ml. Cultures were placed on ice, sonicated to separate mothers from daughters, and cell sizes were measured on a Z2 Coulter Counter. Statistics were performed using a mixture of custom Perl scripts, R and Microsoft Excel.

Glycogen synthase overexpression constructs. High-copy 2uM yeast genome tiling plasmids (Jones, Stalker et al. 2008) YGPM-16i16 (*gsy2*) and YGPM-26p05 (GSY2) were obtained from Aaron Neiman. YGPM-16i16 overlaps the 3' end of the *gsy2* ORF, and the full length of *HSP60*, *LCB5*, *VPS63*, *YPT6* and *TMA7*. YGPM-26p05 contains full length *HSP60*, *GSY2* and *YLR257W* as well as the 5' end of the *lcb5* ORF. These plasmids were transformed into wild-type haploid yeast (both BY4741 and BY4742) and grown in SC-Leu raffinose media to mid-log phase.

Plasmids expressing wild-type and hyperactive glycogen synthase (Pederson, Cheng et al. 2000; Pederson, Wilson et al. 2004; Torija, Novo et al. 2005) were obtained from Jean M. Francois. pGSY2 (pYcDE2-GSY2; 2μM, *TRP1*, *GSY2* CDS under the *ADH1* promoter) and pGSY2Δ643 (pYcDE2-GSY2Δ643; 2μM, *TRP1*, *GSY2* CDS under

ADH1 promoter) were transformed into BF305-15d. Cells were grown in SC-Trp raffinose media to mid-log phase.

For both pairs of plasmids, cells were grown to mid-log phase, placed on ice, and sonicated to break apart clumps. Cell volumes were measured on a Z2 Coulter Counter. At least five transformants from each strain were measured, and the median cell volumes were recorded. Each bar graph in Figure 6 shows the average of all medians; error bars are standard error of the mean (SEM).

2.5 Future Experiments

2.5.1 Induced mobilization of glycogen

If an increase in intracellular glucose derived from mobilization of storage carbohydrates is the driving force for Start in carbon-limited cells, then premature mobilization of glycogen should permit cells to pass through Start at a smaller cell size. An experimental design would be to take small unbudded G1 daughters, and, at different sizes (points in G1) induce glycogen degradation. If glycogen breakdown can be induced at the right time, the resulting burst in glucose should promote Start. Too early, or continuous, liquidation might even delay Start. Liquidation too late (i.e.: immediately after Start) should have no effect. To some extent, this prediction is already addressed by the experiments in which cAMP is added to cells which do, or do not, contain carbohydrate. However, since cAMP has many effects, additional experiments addressing the same point would be valuable.

To create another way of inducing glycogen breakdown on demand, I would use Sga1. Sga1 is a sporulation specific glucoamylase capable of breaking down glycogen. I created a GALpr-SGA1ΔN strain lacking Sga1's vacuolar signal peptide and transmembrane domain with the hope of creating an inducible cytoplasmic Sga1. I integrated the GAL1,10 promoter into the 5' end of SGA1 to truncate the first 63 amino acids of the protein. This removes the transmembrane and vacuolar targeting sequence, as well as most of the poorly conserved N-terminus. I confirmed that the gene is induced by galac-

tose using qPCR (data not shown). Unfortunately, induction of SGA1ΔN did not result in loss of glycogen, as measured by iodine staining (data not shown). One possibility is that I removed too much of the N terminus. It would be interesting to try a smaller truncation. Another option is an inducible constitutively active glycogen phosphorylase (Gph1).

2.5.2 Does induction of Cln/CDK activity promote carbohydrate liquidation?

Glycogen phosphorylase (Gph1), neutral trehalase (Nth1), and the regulatory unit of PKA (Bcy1) might all be Cln/CDK targets. Cln/CDK activity might induce carbohydrate liquidation and PKA activation, resulting in a glycolytic burst and increased ribosome biogenesis. There are several experiments that can be done to probe the "Finishing Kick" hypothesis in more detail. *cln1 cln2 cln3* cells should block in G1 with high glycogen levels, and induction of *GAL-CLN* should induce glycogen degradation and a spike in cAMP.

2.5.3 Generation of phosphorylation site mutants chosen from the computational screen for potential CDK and PKA targets.

The computational screen identified several potential targets of both CDK and PKA. Among these are the two enzymes that degrade storage carbohydrates (Gph1 and Nth1) a transcription factor that regulation cell-cycle entry (Whi5), Securin (Pds1), a transcription factor involved in growth related gene expression (Stb3). Phosphorylation of CDK and PKA sites has been detected by mass-spec for Gph1, Nth1 and Whi5. We will synthesize variants of these genes that lack CDK and/or PKA phosphorylation sites and assay cells for cell-cycle progression, critical size, and carbohydrate levels to determine if dual phosphorylation by CDK and PKA regulate these genes.

Chapter 3. Constructs for measuring PKA activity and glycogen in single cells

There exist several methods for measuring PKA activity and cAMP and glycogen levels in cell populations using enzymatic (cAMP and glycogen) and in vitro phosphorylation (PKA) assays. These methods rely on large numbers of cells which can never be 100% synchronized. Furthermore cAMP is extremely unstable, in part due to the presence of phosphodiesterases, and the concentration of cAMP can change extremely rapidly. There are also in vivo immunohistochemistry methods for measuring phosphorylation of PKA targets (Czernik, Girault et al.) and microscopy methods for measuring glycogen (Schlee, Miedl et al. 2006), neither of which are quantitative, and both of which require fixed cells. Recently a Fluorescence Resonance Energy Transfer (FRET) based PKA activity sensor was developed for use in mammalian cells (Zhang, Ma et al. 2001; Allen and Zhang). A FRET approach has many advantages: it is a single cell assay (obviating the need for synchronized cultures); it is real-time; it deals with living cells. I have cloned the mammalian FRET construct into a yeast vector and successfully used it to measure PKA dynamics throughout the cell-cycle in live single yeast cells. I have also designed a construct that may be able to measure glycogen levels, and to show glycogen localization, in live single cells. It should be possible to use these constructs to investigate changes in PKA activity and glycogen levels.

3.1 Development of a FRET-based sensor of PKA activity in yeast

Cyclic AMP dependent protein kinase (PKA) activity regulates carbon metabolism, cell-cycle progression, the DNA damage checkpoint, and transcription of ~1/6 of the yeast genome (Wang, Pierce et al. 2004). There are several methods for measuring cAMP levels in cell populations. These methods have several drawbacks: they are time consuming, show great lab-to-lab variability, and require large numbers of destroyed cells. In addition, PKA activity is spatially regulated in mammalian cells (Zhang, Ma et al.), and may be so in yeast (Santangelo 2006). The AKAR3 PKA sensor will be able to detect PKA activity with sub-cellular resolution. I cloned the AKAR3 construct into a yeast expression vector and measured PKA activity throughout the cell cycle and in response to a glucose spike (see Figure 9).

3.2 Characterization of pAKAR3 in budding yeast

To observe the cell-cycle dynamics of PKA activity I grew WT haploid yeast on an SC raffinose –ura plate at 30^{o} C, and imaged cells every 10 minutes for six hours on a DeltaVision microscope. Around the time of bud emergence, a sharp increase in PKA activity, followed by a gradual decrease, is clearly visible (Figure 10 A & B) for a single cell and in the average changes for ten cells (Figure 10 C). This result confirms the existence of a spike in PKA activity around Start, and that my reporter works.

Budding yeast growing in glucose de-repressed conditions exhibit a large and rapid burst of cAMP levels following addition of glucose (van der Plaat 1974). To see if I could detect an increase in PKA activity following addition of glucose using the pAKAR3 construct I grew WT diploid yeast with the pAKAR3 plasmid in liquid SC Ethanol (SCE) –ura media, and added glucose to the media to a final concentration of 2%. At 15 and 30 minutes following glucose addition I fixed a fraction of the cells and measured FRET using FretScale (Figure 10 D&E). Fifteen minutes following addition of glucose the FRET signal is significantly higher than cells grown in SCE, and by 30 minutes the signal has significantly decreased, but is still significantly above that of ethanol grown cells. This is qualitatively what I expect based on batch culture cAMP measurements. I have reason to believe that too much AKAR3 is being expressed and is limiting my dynamic range, and possibly the temporal resolution as well. There is a negative correlation (Pearson = -0.27) between absolute AKAR3 expression level in individual cells (measured by the average CFP and YFP signals) and the FRET signal. Additionally, cells expressing high levels of AKAR3 never have high FRET values, while cells expressing low levels have FRET values that are more evenly distributed (data not shown). It is likely that, especially in the high expression cells, not all of the AKAR3 protein in the cell is being phosphorylated. It is also possible that the excess protein is titrating PKA activity.

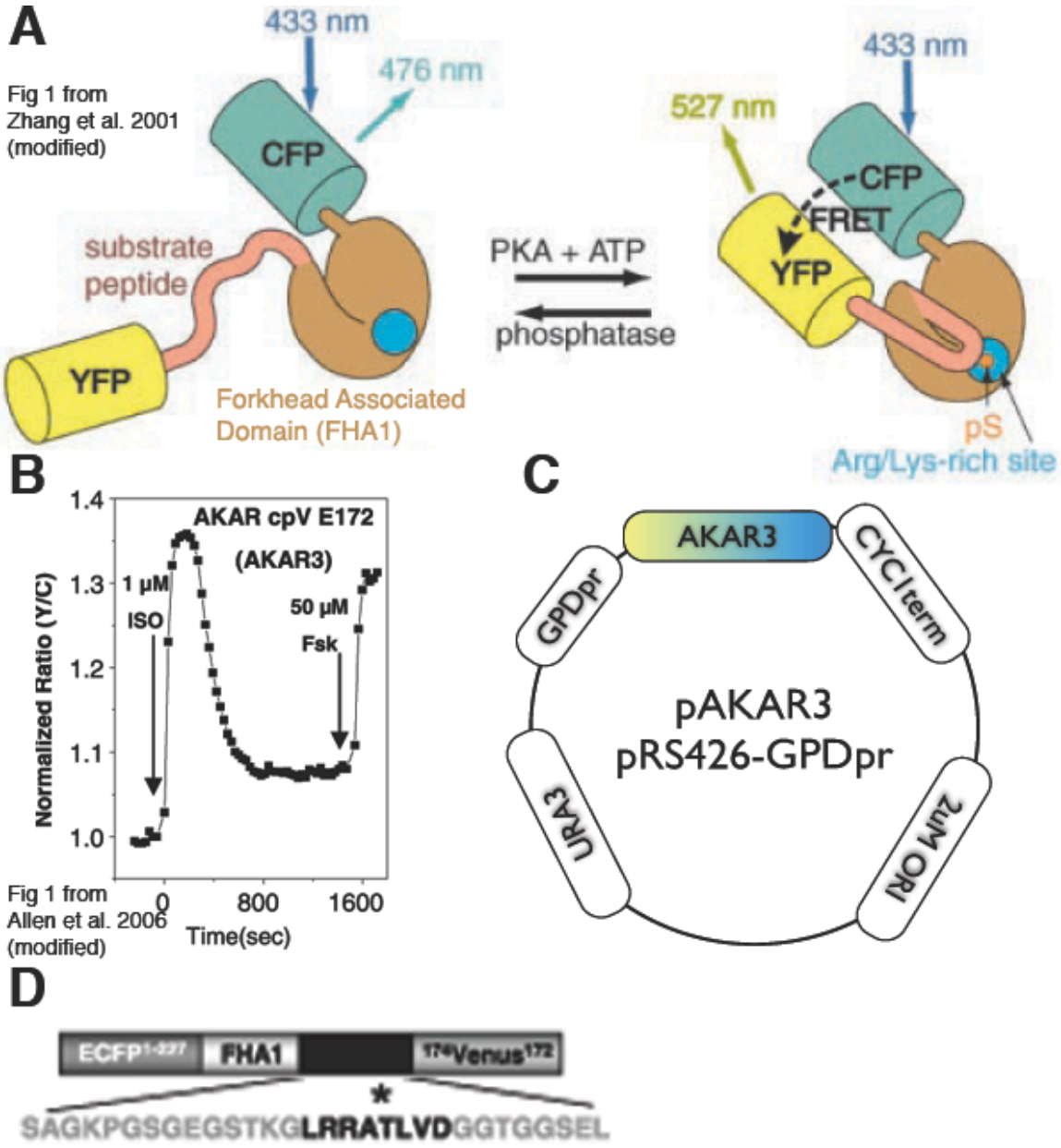

Figure 9. Diagrams of AKAR3 constructs

Diagram of AKAR, the FRET based PKA sensor. The sensor consists of a CFP donor, an FHA1 domain, a 14aa linker and a circularly permuted variant of Venus (Nagai, Yamada et al.) as the acceptor. The unphosphorylated linker is free; following phosphorylation by PKA it interacts with the FHA domain. This brings the CFP and YFP closer together, and increases the FRET (A). The phosphorylation site is shown in detail (D). The change in FRET signal in mammalian cells in response to isoproterenol (ISO) and forskolin from Allen et al (Allen and Zhang) (B). The pAKAR3 construct for expression in yeast, in which AKAR3 is cloned into the pRS426-GPDpr vector(C).

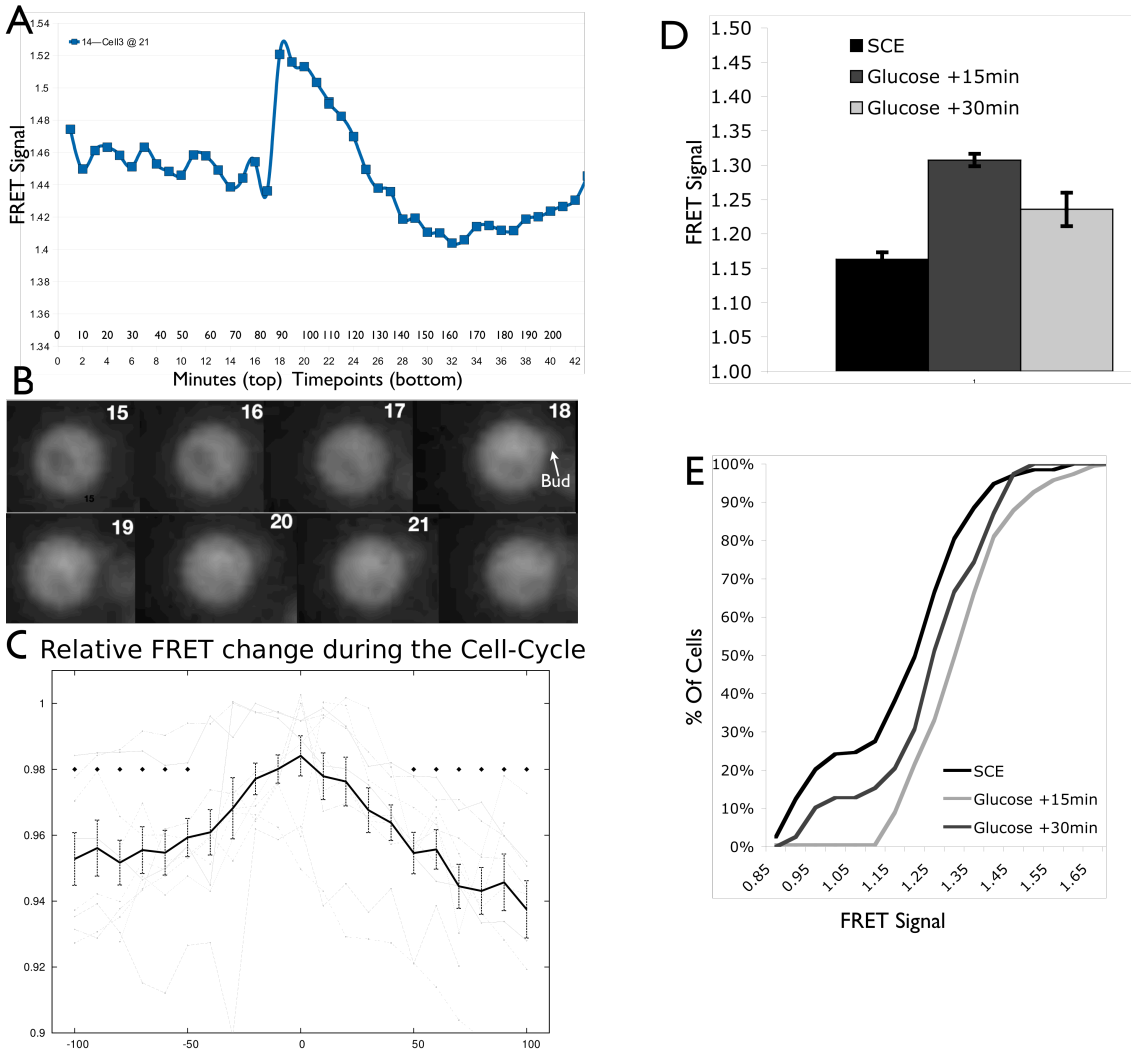

Figure 10. Quantification of GPDpr-AKAR3 construct

Quantification of PKA activity using pAKAR3 in SC Raffinose grown cells (A-C) and SC Ethanol grown cells (D &E). Changes in FRET signal for a single cell is quantified in (A) and images are shown in (B). Cells were normalized so that maximal FRET is 1 for all cells, and time 0 is bud emergence. The average FRET signal of 10 normalized cells is shown in (C). Error bars are SEM and asterisks above the line denote timepoints where the FRET signal is significantly different (t-test) from time 0. FRET values for cells grown in SCE media spiked with glucose. (D) shows average and SEM for cells grown on SCE and 15 or 30minutes following addition of glucose to 2%. The cumulative distribution for the same cells (E). Data for all three conditions are significantly different from each other (t-test).

3.3 Glycogen measurements in single cells

3.3.1 An attempt using periodic-Schiff to measure glycogen in fixed cells

As with cAMP, there is no method for quantitative glycogen measurement in single cells. Brewers use a periodic-Schiff reagent based staining of glycogen to monitor the health of actively fermenting brewing strains (Schlee, Miedl et al. 2006; Chlup, Bernard et al. 2008). This method uses periodic acid, which selectively oxidizes glucose residues to form aldehydes. Schiff reagent reacts with aldehydes and fluoresces, allowing glycogen to be quantified.

I attempted to optimize the staining procedure for use in lab strains and see if this method can be used for quantitative or semi-quantitative single-cell measurements of glycogen. This would have allowed precise measurement of the timing of glycogen breakdown during Start in fixed cells. Unfortunately, this method stains *gsy1 gsy2* cells , which contain no glycogen, quite well (data not shown). Thus Schiff reagent must be staining something else as well. The periodic reagent stains chitin (Graham Stewart. Personal communication); it may be that chitin (or mannan or glucan) staining results in high background. I did not pursue this further.

3.3.2 Monitoring glycogen dynamics in live cells.

To monitor glycogen dynamics in live cells, I designed a construct containing a glycogen binding domain (GBD), GFP and a nuclear localization signal (NLS). This construct is designed to exploit competition between the NLS and the GBD. When glycogen is abundant the GBD should bind glycogen, and the GFP will localize to wherever glycogen is present in the cell. In the absence of glycogen the NLS will dominate, and the GFP will be nuclear. It might be possible to quantify intermediate concentrations of glycogen based on the nuclear/cytoplasmic ratio of GFP.

To construct the plasmid the cloning facility cloned a GFP-NLS construct into an ho::METpr integrating plasmid (Voth, Richards et al. 2001). They then PCR amplified genomic DNA corresponding to the GBD of Gal83 (aa152-251) (Figure 11 A) and cloned

the PCR fragment upstream of the GFP, with 5xGly linker separating the two domains (Figure 11 B).

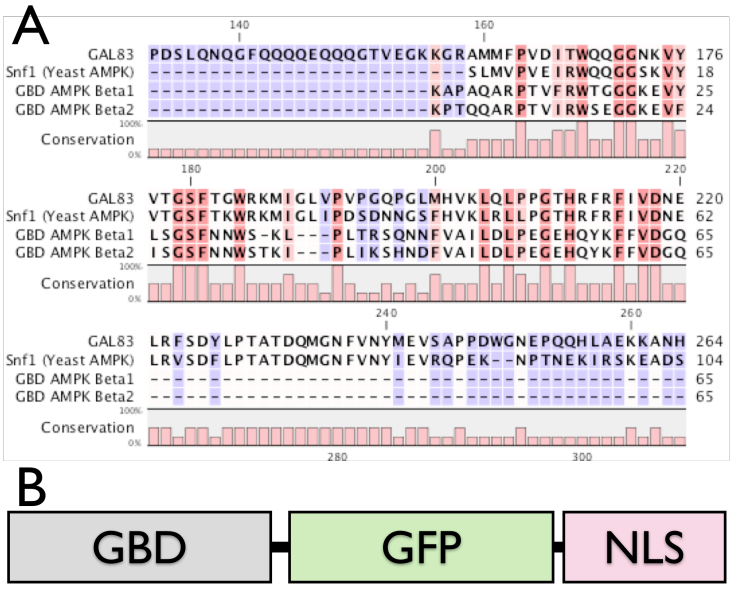

Figure 11. GBD-GFP-NLS construct

The design for a construct to measure real-time glycogen levels in single cells. Alignment of the yeast Gal83 glycogen binding domain to three glycogen binding domains with solved structures (A). Design of the GBD-GFP-NLS construct (B). The construct contains a glycogen binding domain (GBD) fused to a GFP with a C-terminal NLS. The NLS and the GBD will compete with each other. In the absence of glycogen the construct should be nuclear. In the presence of glycogen, some of the construct should remain cytoplasmic and bound to the glycogen. The nuclear/cytoplasmic GFP ratio should be indicative of the amount of glycogen inside the cell.

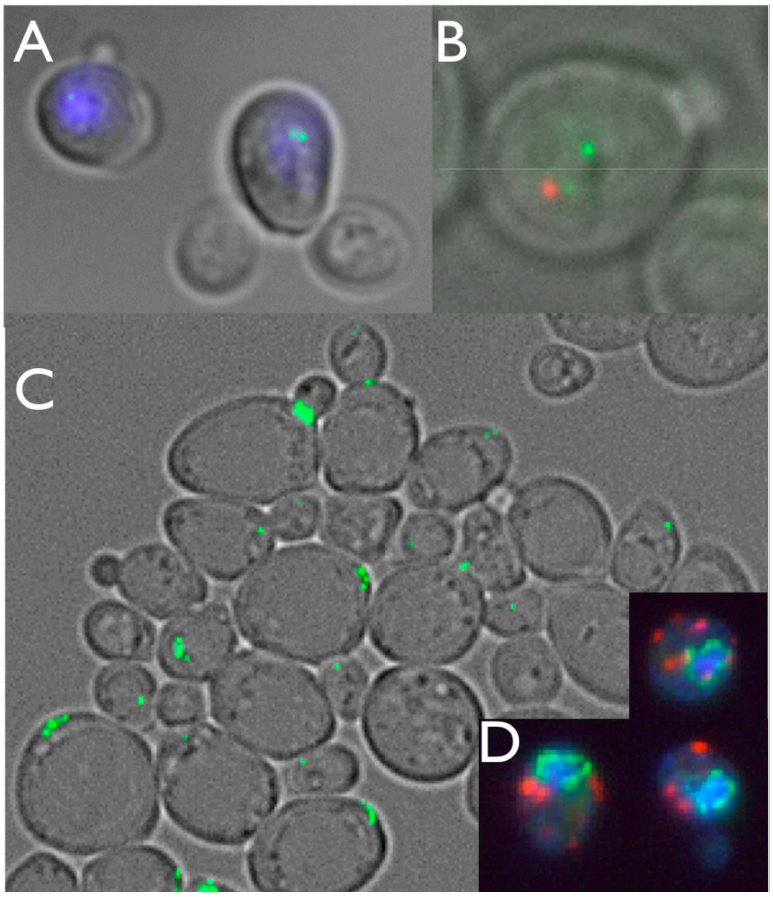

Figure 12. Cells expressing the GBD-GFP-NLS construct

Yeast expressing the GBD-GFP-NLS were grown in SC-Met Glucose (A&B) or SC-Met Ethanol (C). Cells in (B) express Spc42-mCherry to mark the spindle pole body. In the presence of glucose GBD-GFP-NLS is clearly in the nucleus (A). In large ethanol grown cells GBD-GFP-NLS may be cytoplasmic (C). Glycogen phosphorylase is punctate and cytoplasmic (D). Cells in (D) are NUP100-GFP GPH1-RedStar2 and stained with DAPI.

To test the GBD-GFP-NLS construct, cells were grown in SC-Met with either glucose (low glycogen accumulation) or ethanol (high glycogen accumulation) as the carbon source. Cells were fixed and imaged using a GFP filter set at 100x. Cells grown in glucose (Figure 12 A & B) exhibit clearly nuclear puncta. The nuclear puncta are not at the spindle pole body (Figure 12 C). Cells grown in ethanol exhibit far more puncta, and these are probably cytoplasmic (Figure 12 C and data not shown). Glycogen is mostly cytoplasmic and punctate in EM images of yeast, and glycogen phosphorylase is punctate and cytoplasmic (Figure 12 D). I have a version of the construct with two GBDs, which may bind cooperatively to glycogen (David Green, personal communication). Increased affinity for glycogen will tilt the equilibrium towards binding glycogen, and out of the nucleus. The 1x and 2xGBD constructs need to be characterized in both wild-type and glycogen deficient strains before they can be used to measure cell-cycle regulation of glycogen.

3.4 Materials and Methods

Fixed cell fluorescence microscopy For visualization of fluorescent constructs yeast were grown to mid-log phase, washed with PBS, and fixed with 3.7% formaldehyde for 5 min, and washed again with PBS. To mark the nucleus cells were set in mounting medium containing 4,6-diamidino-2-phenylindole (DAPI) (Vectashield; Vector Laboratories, United Kingdom). Images were acquired using a Zeiss Axioplan2 microscope (Carl Zeiss, Thornwood, NY) with a Zeiss mRM Axiocam equipped with a 100X oil objective (Plan-Neofluar, numerical aperture 1.46).

For Glycogen Binding Domain (GBD)-GFP-NLS constructs cells containing the integrated construct were grown overnight in SC-Met media with the relevant carbon source in order to express the METpr-GBD-GFP-NLS construct. Cells were then washed and fixed and stained as described above.

For fixed cell FRET studies cells were grown to early mid-log phase (~0.5 - 1*10^7CPM) in SC-ura Ethanol media. The culture was split into two fractions and glucose was then added to one fraction to a final concentration of 2%. Cells were taken from both fractions at 0, 15 and 30 minutes, placed on ice, sonicated to break up clumps, and fixed in 3.7% formaldehyde. Cells were then washed in PBS and imaged on the Zeiss Axioplan2.

For live cell analysis cells were grow on an SC –ura raffinose agar pad in inverted in a 35mm diameter petri dish with a coverslip glued over a hole drilled in the bottom of the petri dish (MatTek Corporation). Cells were grown to mid-log phase in SC-ura raffinose liquid media, sonicated briefly, and 3ul of cells were placed on the agar pad, which was then inverted to position the cells between the coverslip and agar. Cells were grown on raffinose instead of glycerol or ethanol because glycerol/ethanol grown cells were killed by the low-wavelength light used to excite the CFP (data not shown).

The petri dish was mounted in a thermally insulated temperature-controlled chamber at 30°C. Cells were imaged using a restoration microscope system (DeltaVision RT; Applied Precision) with an inverted microscope (1X-70; Olympus), rapid shutters, and a 60x/1.4 NA lens (planApo; Olympus) using CFP and YFP filters (Chroma Technology Corp.), a Photometrics Cool SNAP HQ camera(Roper Scientific). The DeltaVision RT has a sharp long-pass filter at 420 nm to decrease phototoxicity from blue light during live-cell imaging. Z stacks were obtained every ten minutes for six hours. More frequent timepoints (every 2.5 minutes) killed the cells, presumably due to phototoxicity from the CFP excitation. Deconvolution and FRET calculations were done using SoftWoRx 2.50 (Applied Precision).

FRET Analysis Fixed-cell acquisitions images from the Zeiss were converted to 16-bit Tiff images and renamed using a custom Automator script (Carey & Suda unpublished) and ImageJ (rsbweb.nih.gov/ij/). Images were then analyzed both manually and using FretSCal (Ess, Riffle, and Muller, unpublished), a Matlab script that automatically identifies and analyzes regions with a FRET signal. Manual analysis and FretSCal gave

qualitatively identical results; FretSCal analysis was chosen as it is automated and can quickly scan through hundreds of images in an unbiased manner. FRET values and background corrected fluorescence intensities for regions of interest automatically identified by FretSCal were collected for further analysis.

Live-cell images collected from the DeltaVisionRT were analyzed using SoftWoRx. To correct for the large level of cell-to-cell variation in pAKAR3 expression FRET ratios for each cell were normalized so that the highest FRET ratio for each cell over a given cell cycle was set to one. To facilitate comparison between cells, the time point at which bud emergence was first visible was set to 0. FRET ratios for multiple cells were obtained from SoftWoRx and the average and standard error of the mean for each time point, relative to budding, was calculated.

pAKAR3 Plasmid Construction. To obtain real-time single-cell PKA activity measurements in yeast I obtained the AKAR3 PKA activity sensor from Jin Zhang in the pCDNA3.1 vector under the control of the CMV promoter with a $G418^R$ marker (See Figure 9 A,B,D). The expression level of the AKAR3 construct is critical: too high a level, and the protein might titrate out PKA activity, not become fully phosphorylated, or both; too low and the fluor will not be visible. I started on the low end of the expression spectrum and transformed the CMVpr-AKAR3 construct directly into yeast and selected several random genomic integrants, which where confirmed by PCR and the cell's inability to lose the construct in the absence of selection (data not shown). I was unable to see a signal in any transformants. I then moved to the high end of expression, and sub-cloned the AKAR3 ORF into the pRS416-GPDpr plasmid (Figure 9 C), a high copy, high expression vector (Mumberg, Muller et al. 1995).

3.5 Future Directions

3.5.1 Further characterization of AKAR3 and cAMP in yeast

The AKAR3 construct exhibits changes in FRET as expected from batch culture measurements of cAMP levels in yeast. The expression level of the current construct is too high, and it needs to be reduced. I will clone the AKAR3 construct under the control

of a few variants of the *TEF1* promoter in a yeast integrating plasmid (Nevoigt, Kohnke et al. 2006). I will then measure FRET ratio in WT and carbohydrate null cells to see if liquidation of storage carbohydrates is required for the spike in cAMP levels.

3.5.2 Confirmation of the GBD-GFP-NLS constructs

I have 1xGBD and 2xGBD constructs in yeast integrating vectors. I will transform each into wild-type, *gph1* and *gsy1 gsy2* strains, all of which I have, and observe GFP localization in glucose and ethanol grown cells. Expression from the *MET* promoter is relatively weak and GFP signal is not far above background. I should be able to use the confocal or the more sensitive camera to get better images. If the constructs do indeed work, it may be possible to visualize both the cAMP spike and glycogen liquidation in the same cells. To do this I would need a red version of the GBD construct, but that could be synthesized quite easily.

Chapter 4. What would cells without size control look like?

4.1 Background & Introduction

All cells coordinate increase in mass with cell division. Yeast cells link growth and replication through both a sizer and a timer. Metazoan cells are influenced by a combination of intracellular and extracellular signals that control cell growth and cell division, though no molecular sizer or timer has been identified. Here we ask, using simulations of cell growth and division, what would a population of cells look like in which growth and division are unlinked, linked through a timer only, linked through a sizer only, or in which cell growth and division are linked through both a timer and a sizer. We find that size control is required for exponentially growing cells to maintain a biologically reasonable distribution of cell volumes. This is true even if the size control is cryptic -- that is, if most cells are born larger than critical size and are uninfluenced by the sizer. We propose that all cells, microbial and metazoan, must link cell growth and division through some form of size control.

Cell growth, as measured by protein content (Vanoni, Rossi et al. 2005; Porro, Vai et al. 2009) RNA content (Elliott and McLaughlin 1978), the rate of protein production (Bean, Siggia et al. 2006; Di Talia, Skotheim et al. 2007; Talia, Skotheim et al. 2007),or cell volume (Woldringh, Huls et al. 1993) increases exponentially in budding yeast. Within a population the coefficient of variation in the rate of growth and in the amount of time required to complete a cell cycle is somewhere between 0.5 (Woldringh, Huls et al. 1993) and 0.15 (Di Talia, Skotheim et al. 2007). Given this level of variability, how does a population of cells under steady-state conditions maintain size homeostasis? In other words, how does the population as a whole maintain identical mass and number doubling times when both growth and division cycles exhibit large levels of noise?

4.2 Variation in growth rate is constant throughout the cell cycle

Yeast cells exhibit cell-to-cell variation in both growth rate and cell cycle time (Lord and Wheals 1981; Woldringh, Huls et al. 1993; Di Talia, Skotheim et al. 2007). In order to simulate a growing population I need to know the growth rate and the variance. To see if the variance in growth rate changes with time or cell size I generated a synchronous population of YP+Ethanol (YPE) grown G1 daughters by centrifugal elutriation and measured cell volume and population variance with respect to time (Figure 13 A). Cell volumes increases with time as the cells grow during the cell cycle (Figure 13 B triangles). The standard deviation of the population increases (Figure 13 B squares) but the coefficient of variation (CV) remains constant (Figure 13B Xs). These data suggest that the variance in growth rate is constant throughout the cell cycle, and that the standard deviation in cell volume increases because the cell volume is increasing.

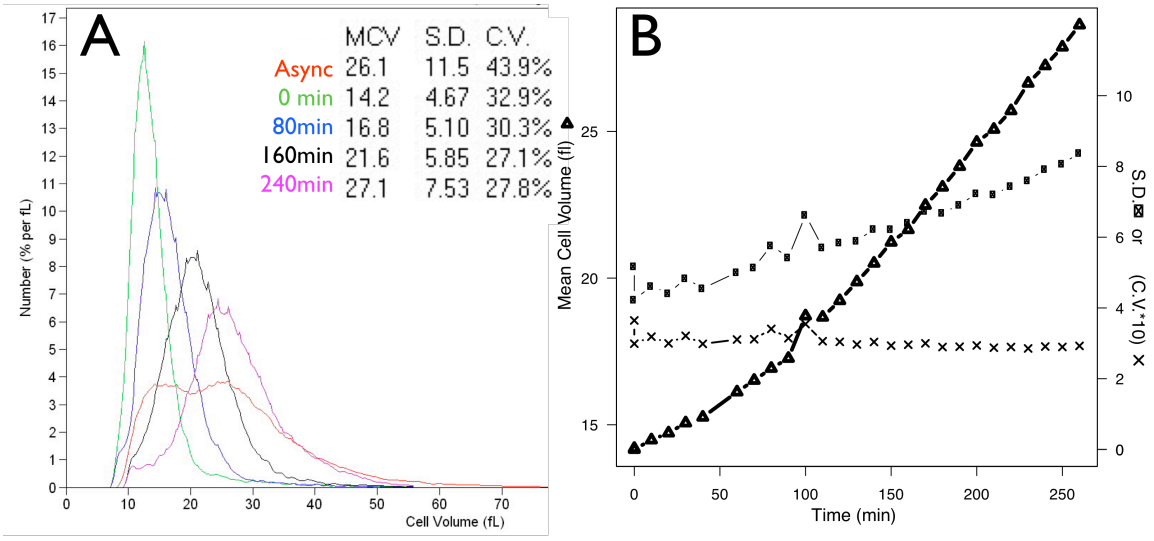

Figure 13. The change in cell volume and population size variance during the cell-cycle

The distribution of cell sizes in a population of cells widens, but coefficient of variation remains constant. Small unbudded G1 cells were obtained by centrifugal elutriation and grown in YPE. Cell volumes were recorded every 10 minutes once the first bud was observed. The distribution of cell volumes for the asynchronous and for the elutriated population at select time points are shown in (A). Mean Cell Volume (MCV) , the Standard Deviation of cell volumes within the population (SD) and the Coefficient of Variation of cell volumes (CV) are shown in (A). These three variables (MCV (triangles), SD (boxes) and CV (Xs)) are graphed for all timepoints in (B).

To confirm that the variance in growth rate is constant, that I have truely measured both growth and variance parameters and not some unknown parameter, and that these two parameters define yeast growth, I generated an in silico population using these parameters and compared it to the data from real yeast. I grew this population with various parameter sets to test this hypothesis. The simplest possibility is that there is no variance in growth – that all cells in the population grow at the same rate (Figure 14 B). The output of this simulation does not match the behavior of real yeast (Figure 13 A) and can be rejected; a population of cells with an identical growth rate exhibits too high a level of size synchrony (Compare Figure 14 B to solid lines in Figure 14 C). The second hypothesis is that the growth rate for each cell is drawn from a normal distribution, and that this growth rate is constant during the cell-cycle (Figure 14 B). This simulation produces results identical to real cells (Compare Figure 14 C solid and dashed lines) showing that, from elutriation data, we can accurately estimate the growth rate and variance of the population, and that these parameters suffice to define the observed pattern of cell growth.

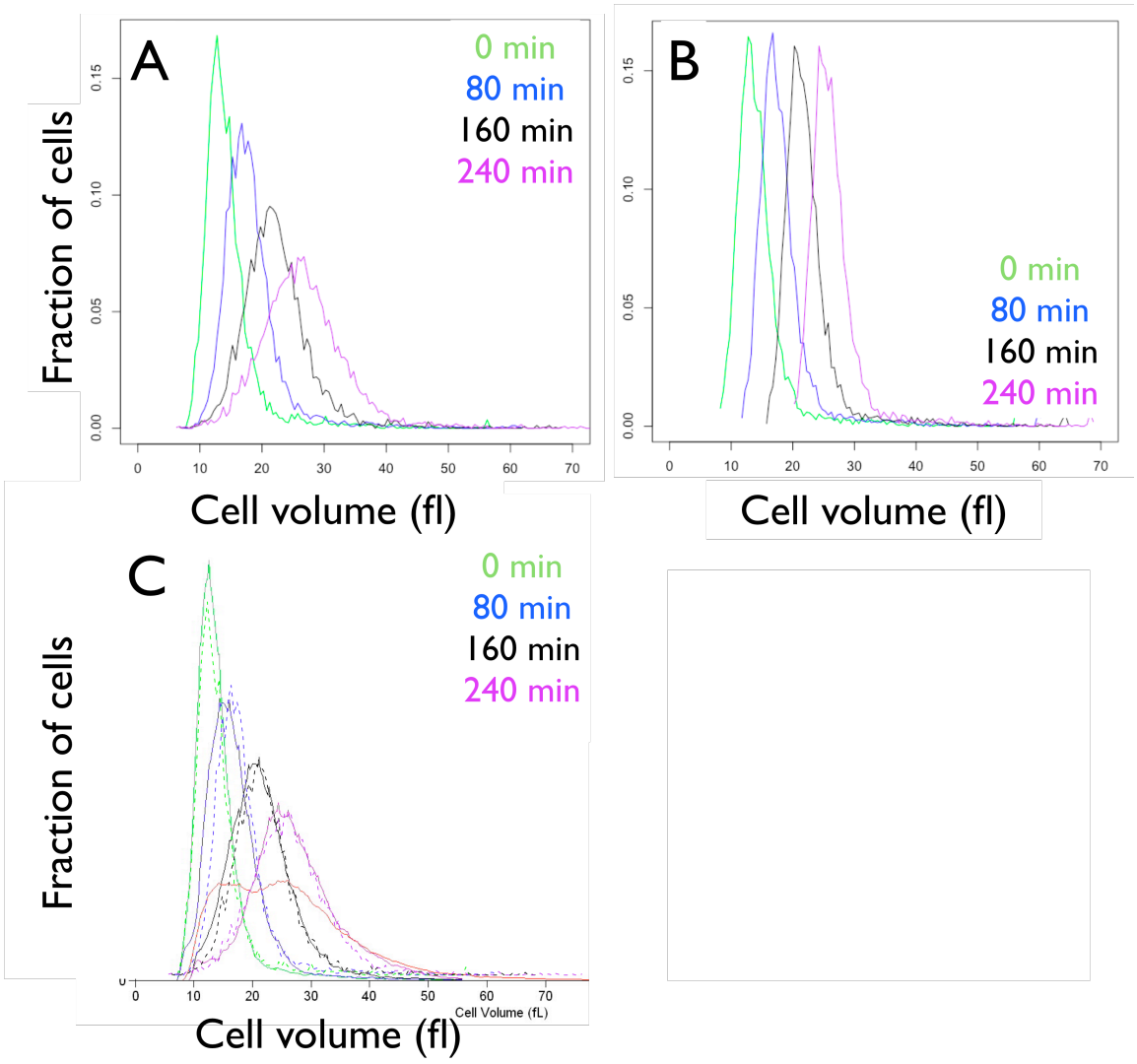

Figure 14. Growth rate variance in real and simulated populations.

Real (Solid lines in C) and in silico (A & B, dashed lines in C) populations of yeast were generated and grown for four hours. Shown are the cell volume distributions for cells whose population growth rate variance is fit to real cells (A) and a population lacking variance in growth rate (B). (C) shows an overlay of the real and in silico populations. In silico populations were grown with a population doubling time of 250min and a growth rate variance of 0.3.

4.3 Cell growth is exponential

Historically budding yeast growth has been measured as exponential. However recent evidence suggests that growth might be linear with multiple Rate Change Points (RCP) due to changes in the actin cytoskeleton (Goranov, Cook et al. 2009). I measured the growth rate in various elutriated cultures and, consistent with Goranov et al, found the linear model with rate change points to be a slightly better fit than exponential; both fits are significantly better than the single linear curve (Figure 15). The differences in fit are slight; within a short region exponential and linear curves are nearly identical. In addition the placement of RCPs in (Figure 15 B) does not correspond to the same cell-cycle landmarks as in Goranov et al (data not shown). In my hands, in cells coming out of the elutriator, growth is most likely exponential.

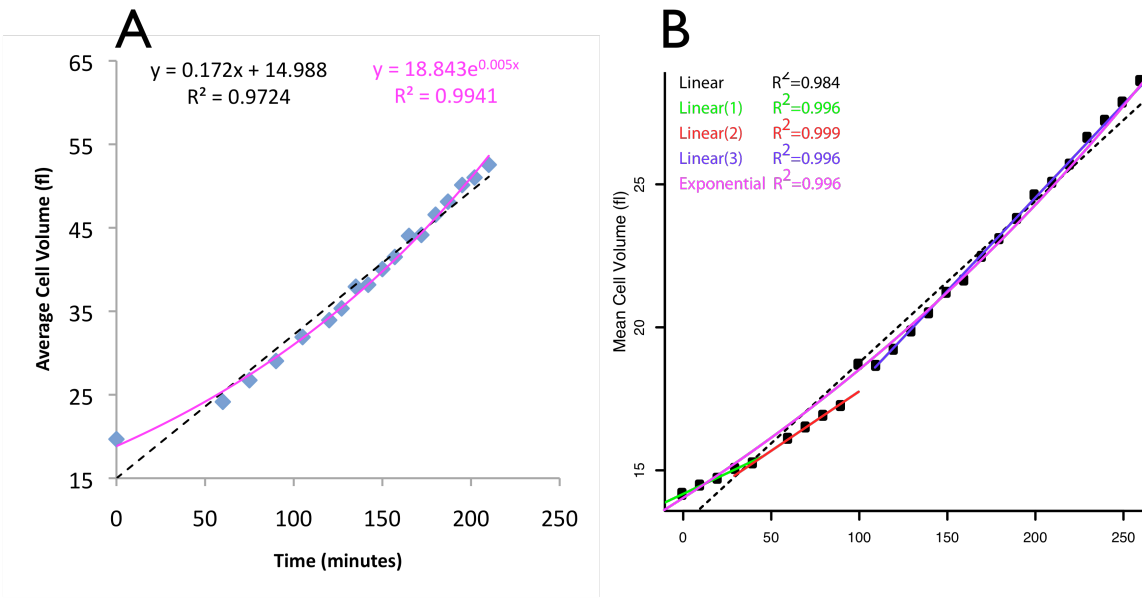

Figure 15. Budding yeast may grow linearly with rate change points

Elutriated cells were grown and volume was measured every ten minutes. The exponential fit (purple) is better than the single linear fit (black dashed line). Three separate linear fits provide the best fit in (B); it is not clear where to place the RCPs in (A).

4.4 The probability of budding depends on the time or size spent in G1

The probability of a cell passing through Start depends on both cell volume and the time spent in G1 (Tyson, Lord et al. 1979; Lord and Wheals 1981). Using the in silico yeast one can ask what a population of cells would look like if which passage through Start were completely random (the probability of budding for each cell is constant and independent of time and size). I find that if bud emergence is not dependent on cell volume the results of an elutriation look completely different from what is seen in real yeast (Figure 16). For elutriation to function as a means of cell-cycle synchronization, cells must have size control.

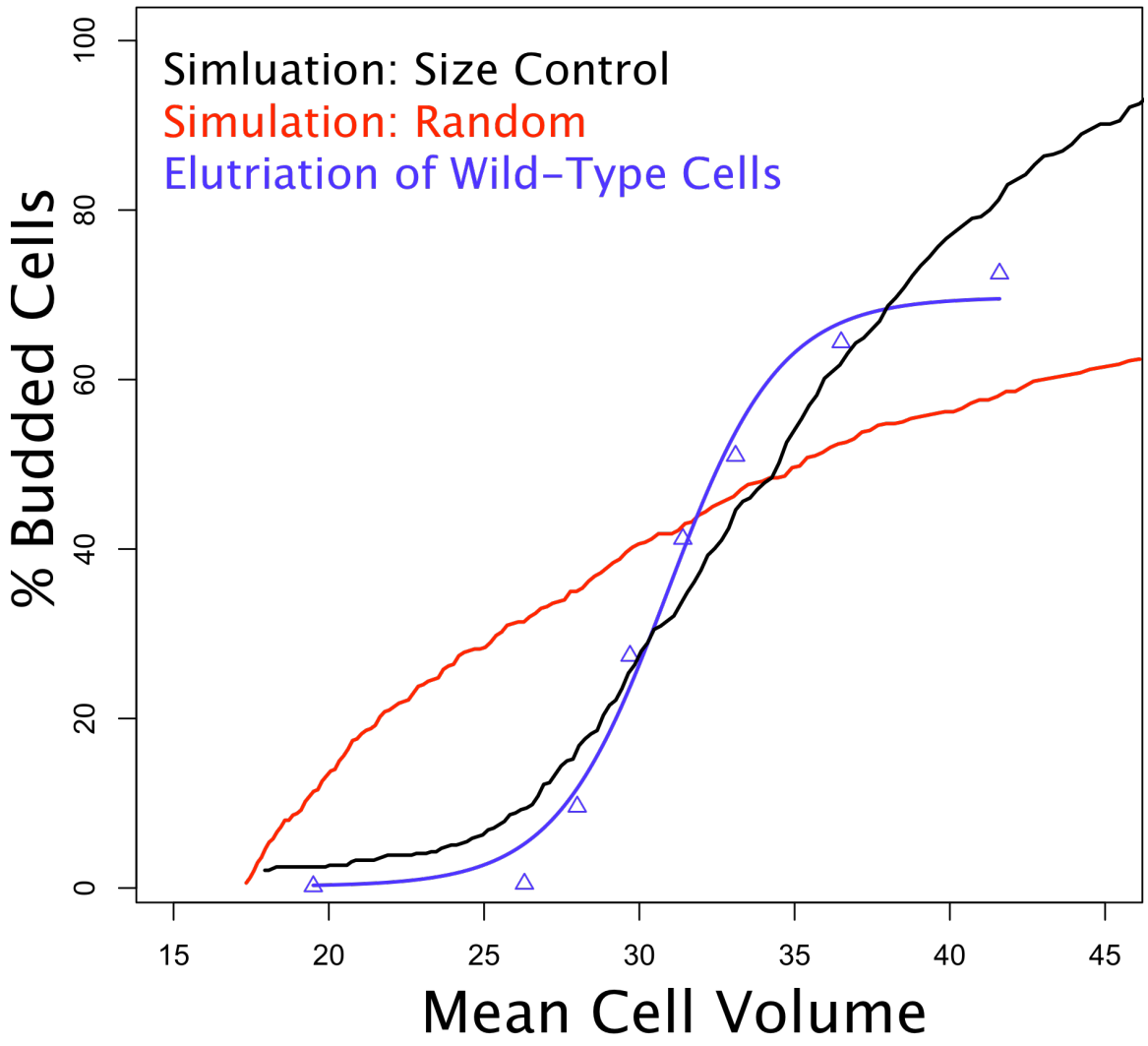

Figure 16. Fraction of budded cells in simulations of yeast with and without size control as compared to a real elutriation of wild-type yeast

Wild-type small unbudded G1 cells were obtained by elutriation and budding and cell volume were monitored (blue triangles) and fit to Equation 2 (blue line). An in silico elutriation as seeded using data from the first timepoint. Two in silico elutriations were performed. In one budding was regulated size (black line). In the second cells bud randomly (budding is not influenced by cell volume) (red line).

4.5 Exponentially and linearly growing cells require size control

To investigate the effects of growth rate (linear vs exponential) and size control, I simulated populations with different growth rates and methods of control over Start (Figure 17). Both exponentially and linearly growing populations lacking size control exhibit excessively broad size distributions. This suggests that size control may be necessary even for linearly growing populations to maintain the observed cell size distribution.

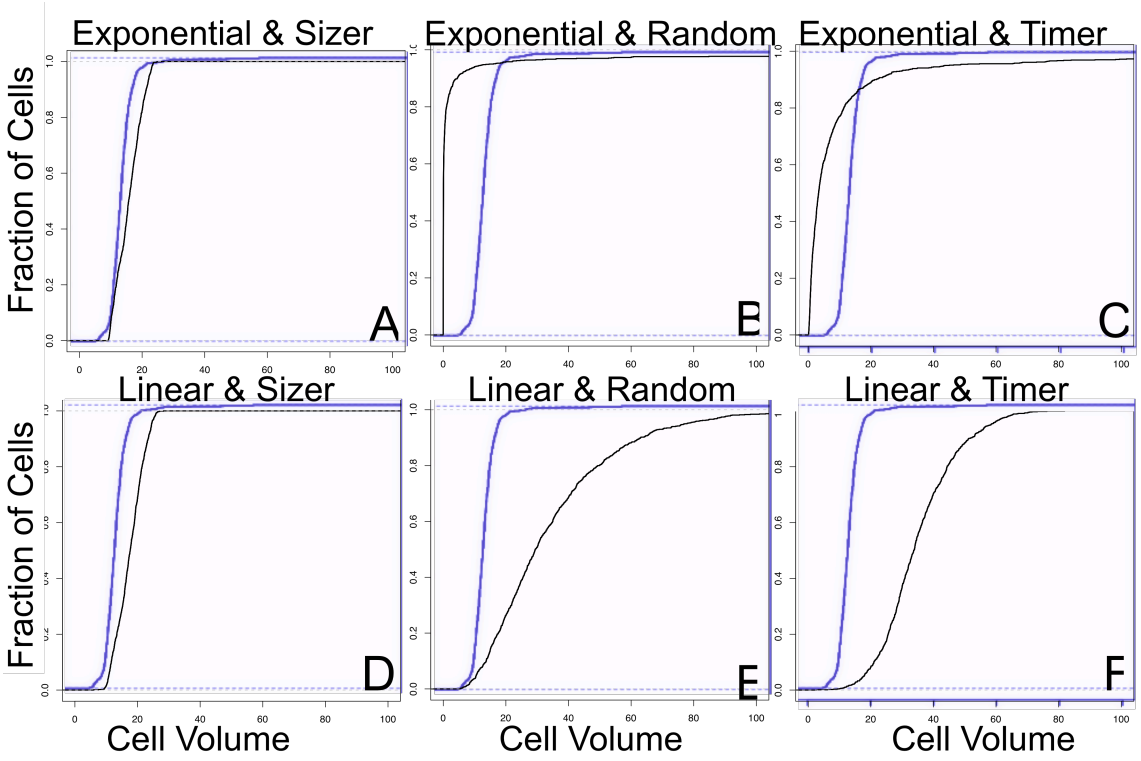

Figure 17. Growth and Start control effects on the size distribution in in silico yeast populations

Identical cell size starting populations were taken from a real elutriation, and in silico yeast were grown for ~15 doublings with either linear (D, E, F) or exponential growth (A, B, C), and either sizer (A, D), timer (C, F), or random (B, E) control over Start. The real asynchronous population fromß which the elutriated fraction was taken is shown (blue). The size control linear (D) and exponential (A) simulations provide the best fit to the real yeast. Linear populations that lack size control exhibit a slight spreading of the size of the population towards large and small cells due to cell-to-cell variance in the growth rate. Exponential populations that lack size control exhibit extreme variation in size within a population. All simulated cells have the same population doubling time.

4.6 Discussion and future directions:

The idea that exponentially growing yeast must have size control to prevent large cells from getting progressively larger, and small cells from getting progressively smaller, is an old idea (Bell and Anderson 1967; Bell 1968). The advantage of my simulations is that they can be fit to data, and used to measure cell-to-cell variability in both growth rates and size control fidelity in real populations of cells. My simulations suggest that linearly growing yeast also require size control to maintain population distributions similar to those seen in wild populations. This is markedly different from current state of the field in which it is thought that only exponentially growing cells require size control (Cooper 2004; Cooper 2006).

The simulator is currently functional, but lacks a framework for the introduction of, and automated fitting to, real data. This makes using the simulator to analyze real populations tedious; this processes needs to be improved. Following this addition, it will be trivial to use the simulator to investigate the fidelity of size control in different mutants in all of our existing elutriation data.

There are two immediately attractive uses of the simulator. The first will be to use the simulator to estimate how sloppy size control is in various mutants. This can be done in single cells, but the simulator will allow us to come up with a population wide estimate. The second is to combine the timer and sizer models in the simulator. The daughter-specific G1 delay (Laabs 2003) is responsible for all of G1 in most glucose grown daughters (Di Talia, Wang et al. 2009). It will be interesting to see if integration of the timer and sizer for control of Start is required to fit the simulator to the data.

4.7 Materials and Methods

The in silico yeast simulator was written in Perl. Graphs were created in R. There are several stages to the simulation.

4.7.1 User defined parameters

On the command line the user specifies several parameters. Among them are: (1) linear or exponential growth (2) the population doubling time (3) The mechanism for start control (sizer, timer or random) (4) the population size (5) the length of time for the simulation to run (6) the initial distribution of cell volumes.

4.7.2 Seeding of in silico chemostat

The simulator has two methods for generating the initial yeast population. The simulator either reads a cell volume distribution from a file generated by the Z2 Coulter Counter or generates a normally distributed population of cell volumes with a user specified mean and variance.

4.7.3 Running the simulator

Each cell is simulated as an independent object, with its own properties (age, volume, growth rate, etc). Following cell division, the daughter receives 40% of the total volume and replaces a randomly chosen cell within the population, so that the population size remains constant. Aside from volume, all of the properties of the daughter are reset, and a new cell-specific growth rate is chosen for that daughter. During the run the simulator outputs all interesting statistics, such as the percent of budded cells, the fraction of mothers and daughters, the volume distribution, and the times spent in each phase of the cell cycle.

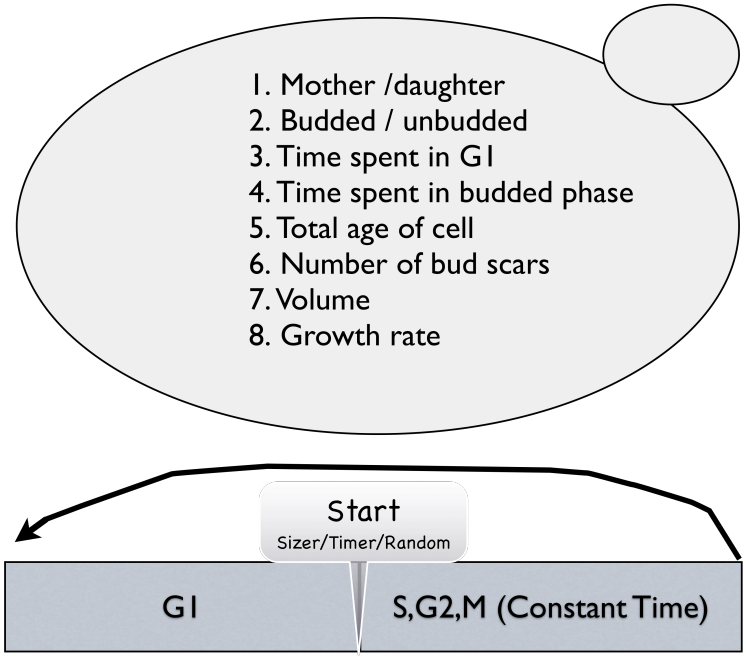

Figure 18. Schematic of yeast simulator

Each in silico yeast cell has several properties associated with it. Each yeast cell begins in G1, and passes through Start whenever the specified criterion (size, time or random) is met. The cell then spends a constant amount in time in the budded phase. The user specifies the population doubling time and the growth rate of each cell is chosen randomly, with user specified variance, to match this doubling time. Eight properties can be obtained from every cell at every timepoint for use in analysis.

Works Cited

Allen, M. and J. Zhang (2006). "Subcellular dynamics of protein kinase A activity visualized by FRET-based reporters☆." Biochemical and Biophysical Research Communications **348**(2): 716-721.

Amberg, D., D. Burke, et al. (2005). Methods in Yeast Genetics: A Cold Spring Harbor Laboratory Course Manual, Cold Spring Harbor Laboratory Press.

Baroni, M. D., P. Monti, et al. (1994). "Repression of growth-regulated G1 cyclin expression by cyclic AMP in budding yeast." Nature **371**(6495): 339-342.

Bean, J., E. Siggia, et al. (2006). "Coherence and Timing of Cell Cycle Start Examined at Single-Cell Resolution." Molecular Cell **21**(1): 3-14.

Bell, G. I. (1968). "Cell growth and division. 3. Conditions for balanced exponential growth in a mathematical model." Biophys J **8**(4): 431-444.

Bell, G. I. and E. C. Anderson (1967). "Cell growth and division. I. A mathematical model with applications to cell volume distributions in mammalian suspension cultures." Biophys J **7**(4): 329-351.

Bernstein, K. A., F. Bleichert, et al. (2007). "Ribosome biogenesis is sensed at the Start cell cycle checkpoint." Mol Biol Cell **18**(3): 953-964.

Blumenthal, R. (1930). "Mitotic Development of Arbacia Eggs in Cyanides." Physiological Zoology **3**(4): 539-563

Bodenmiller, B., J. Malmstrom, et al. (2007). "PhosphoPep--a phosphoproteome resource for systems biology research in Drosophila Kc167 cells." Mol Syst Biol **3**: 139.

Budovskaya, Y., J. Stephan, et al. (2005). "An evolutionary proteomics approach identifies substrates of the cAMP-dependent protein kinase." Proc Natl Acad Sci USA.

Bullough, W. S. and M. Johnson (1951). "The Energy Relations of Mitotic Activity in Adult Mouse Epidermis." Proceedings of the Royal Society of London. Series B, Biological Sciences **138**(893): 562-575.

Burns, V. W. (1956). "Temporal studies of cell division. I. The influence of ploidy and temperature on cell division in S. cerevisiae." J Cell Physiol **47**(3): 357-375.

Byers, B. and L. Goetsch (1974). "Duplication of spindle plaques and integration of the yeast cell cycle." Cold Spring Harb Symp Quant Biol **38**: 123-131.

Byers, B. and L. Goetsch (1975). "Behavior of spindles and spindle plaques in the cell cycle and conjugation of Saccharomyces cerevisiae." J Bacteriol **124**(1): 511-523.

Byers, B. and L. Sowder (1980). "Gene-Expression in the Yeast-Cell Cycle." Journal of Cell Biology **87**(2): A6-A6.

Chang, E. J., R. Begum, et al. (2007). "Prediction of cyclin-dependent kinase phosphorylation substrates." PLoS ONE **2**(7): e656.

Chlup, P. H., D. Bernard, et al. (2008). "Disc stack centrifuge operating parameters and their impact on yeast physiology." Journal of the Institute of Brewing **114**(1): 45-61.

Cooper, S. (1979). "A unifying model for the G1 period in prokaryotes and eukaryotes." Nature **280**(5717): 17-19.

Cooper, S. (2004). "Control and maintenance of mammalian cell size." BMC Cell Biol **5**(1): 35.
Cooper, S. (2006). "Distinguishing between linear and exponential cell growth during the division cycle: single-cell studies, cell-culture studies, and the object of cell-cycle research." Theoretical biology & medical modelling **3**: 10.
Cooper, S. (2006). "Distinguishing between linear and exponential cell growth during the division cycle: single-cell studies, cell-culture studies, and the object of cell-cycle research." Theor Biol Med Model **3**: 10.
Costanzo, M., J. Nishikawa, et al. (2004). "CDK Activity Antagonizes Whi5, an Inhibitor of G1/S Transcription in Yeast." Cell **117**(7): 899-913.
Costanzo, M., O. Schub, et al. (2003). "G1 transcription factors are differentially regulated in Saccharomyces cerevisiae by the Swi6-binding protein Stb1." Mol Cell Biol **23**(14): 5064-5077.
Cross, F. R. (1988). "DAF1, a mutant gene affecting size control, pheromone arrest, and cell cycle kinetics of Saccharomyces cerevisiae." Mol Cell Biol **8**(11): 4675-4684.
Cross, F. R. and C. M. Blake (1993). "The yeast Cln3 protein is an unstable activator of Cdc28." Mol Cell Biol **13**(6): 3266-3271.
Czernik, A. J., J. A. Girault, et al. (1991). "Production of phosphorylation state-specific antibodies." Methods Enzymol **201**: 264-283.
Danaie, P., M. Altmann, et al. (1999). "CLN3 expression is sufficient to restore G1-to-S-phase progression in Saccharomyces cerevisiae mutants defective in translation initiation factor eIF4E." Biochem J **340 (Pt 1)**: 135-141.
de Bruin, R. A. M., W. H. McDonald, et al. (2004). "Cln3 activates G1-specific transcription via phosphorylation of the SBF bound repressor Whi5." Cell **117**(7): 887-898.
Di Talia, S., J. M. Skotheim, et al. (2007). "The effects of molecular noise and size control on variability in the budding yeast cell cycle." Nature **448**(7156): 947-951.
Di Talia, S., H. Wang, et al. (2009). "Daughter-specific transcription factors regulate cell size control in budding yeast." PLoS Biol **7**(10): e1000221.
Dirick, L., T. Moll, et al. (1992). "A central role for SWI6 in modulating cell cycle Start-specific transcription in yeast." Nature **357**(6378): 508-513.
Elliott, S. G. and C. S. McLaughlin (1978). "Rate of macromolecular synthesis through the cell cycle of the yeast Saccharomyces cerevisiae." Proc Natl Acad Sci USA **75**(9): 4384-4388.
Evans, T., E. T. Rosenthal, et al. (1983). "Cyclin: a protein specified by maternal mRNA in sea urchin eggs that is destroyed at each cleavage division." Cell **33**(2): 389-396.
François, J. and J. L. Parrou (2001). "Reserve carbohydrates metabolism in the yeast Saccharomyces cerevisiae." FEMS Microbiology Reviews **25**(1): 125-145.
Futcher, B. (1999). "Cell cycle synchronization." Methods in cell science : an official journal of the Society for In Vitro Biology **21**(2-3): 79-86.
Futcher, B. (2006). "Metabolic cycle, cell cycle, and the finishing kick to Start." Genome Biol **7**(4): 107.
Futcher, B. (2009). "TgI4 lipase: a big fat target for cell-cycle entry." Mol Cell **33**(2): 143-144.

Gallego, C., E. Gari, et al. (1997). "The Cln3 cyclin is down-regulated by translational repression and degradation during the G1 arrest caused by nitrogen deprivation in budding yeast." EMBO J **16**(23): 7196-7206.
Goranov, A. I., M. Cook, et al. (2009). "The rate of cell growth is governed by cell cycle stage." Genes & Development **23**(12): 1408-1422.
Gross, E., D. Goldberg, et al. (1992). "Phosphorylation of the S. cerevisiae Cdc25 in response to glucose results in its dissociation from Ras." Nature **360**(6406): 762-765.
Guillou, V., L. Plourdeowobi, et al. (2004). "Role of reserve carbohydrates in the growth dynamics of." FEMS Yeast Research **4**(8): 773-787.
Hall, D. D., D. D. Markwardt, et al. (1998). "Regulation of the Cln3-Cdc28 kinase by cAMP in Saccharomyces cerevisiae." EMBO J **17**(15): 4370-4378.
Hammerling, J. (1953). "Nucleo-cytoplasmic relationships in the development of Acetabularia." J. Intern. Rev. Cytol **2**: 475-498.
Hartmann, M. (1926). "Über experimentelle Unsterblichkeit von Protozoen-Individuen." Naturwissenschaften **14**(19): 433-435.
Hartwell, L. H., J. Culotti, et al. (1974). "Genetic control of the cell division cycle in yeast." Science **183**(4120): 46-51.
Holt, L. J., B. B. Tuch, et al. (2009). "Global analysis of Cdk1 substrate phosphorylation sites provides insights into evolution." Science **325**(5948): 1682-1686.
Honey, S., B. L. Schneider, et al. (2001). "A novel multiple affinity purification tag and its use in identification of proteins associated with a cyclin-CDK complex." Nucleic Acids Res **29**(4): E24.
Hsu, T. C. (1954). "Mammalian chromosomes in vitro. IV. Some human neoplasms." J Natl Cancer Inst **14**(4): 905-933.
Huang, D., S. Kaluarachchi, et al. (2009). "Dual regulation by pairs of cyclin-dependent protein kinases and histone deacetylases controls G1 transcription in budding yeast." PLoS Biol **7**(9): e1000188.
Hubler, L., J. Bradshaw-Rouse, et al. (1993). "Connections between the Ras-cyclic AMP pathway and G1 cyclin expression in the budding yeast Saccharomyces cerevisiae." Mol Cell Biol **13**(10): 6274-6282.
Jagadish, M. N. and B. L. Carter (1977). "Genetic control of cell division in yeast cultured at different growth rates." Nature **269**(5624): 145-147.
Johnston, G. C., J. R. Pringle, et al. (1977). "Coordination of growth with cell division in the yeast Saccharomyces cerevisiae." Exp Cell Res **105**(1): 79-98.
Jones, G. M., J. Stalker, et al. (2008). "A systematic library for comprehensive overexpression screens in Saccharomyces cerevisiae." Nat Methods **5**(3): 239-241.
Jorgensen, P., J. L. Nishikawa, et al. (2002). "Systematic identification of pathways that couple cell growth and division in yeast." Science **297**(5580): 395-400.
Klein, C. and K. Struhl (1994). "Protein kinase A mediates growth-regulated expression of yeast ribosomal protein genes by modulating RAP1 transcriptional activity." Mol Cell Biol **14**(3): 1920-1928.
Kuenzi, M. T. and A. Fiechter (1969). "Changes in carbohydrate composition and trehalase-activity during the budding cycle of Saccharomyces cerevisiae." Arch Mikrobiol **64**(4): 396-407.

Kuenzi, M. T. and A. Fiechter (1972). "Regulation of carbohydrate composition of Saccharomyces cerevisiae under growth limitation." Arch Mikrobiol **84**(3): 254-265.

Kurat, C. F., H. Wolinski, et al. (2009). "Cdk1/Cdc28-dependent activation of the major triacylglycerol lipase Tgl4 in yeast links lipolysis to cell-cycle progression." Mol Cell **33**(1): 53-63.

Laabs, T. L. (2003). "ACE2 is required for daughter cell-specific G1 delay in Saccharomyces cerevisiae." Proc Natl Acad Sci USA **100**(18): 10275-10280.

Ledvij, M. (2003). "Curve Fitting Made Easy." The Industrial Physicist **9**(2): 24-27.

Lemaire, K., S. Van de Velde, et al. (2004). "Glucose and sucrose act as agonist and mannose as antagonist ligands of the G protein-coupled receptor Gpr1 in the yeast Saccharomyces cerevisiae." Mol Cell **16**(2): 293-299.

Lin, K., P. Hwang, et al. (1995). "Mechanism of Regulation in Yeast Glycogen Phosphorylase." Journal of Biological Chemistry.

Lin, K., P. K. Hwang, et al. (1997). "Distinct phosphorylation signals converge at the catalytic center in glycogen phosphorylases." Structure **5**(11): 1511-1523.

Lin, K., V. L. Rath, et al. (1996). "A protein phosphorylation switch at the conserved allosteric site in GP." Science **273**(5281): 1539-1542.

Lord, P. G. and A. E. Wheals (1981). "Variability in individual cell cycles of Saccharomyces cerevisiae." Journal of Cell Science **50**: 361-376.

Martin, D. E., A. Soulard, et al. (2004). "TOR regulates ribosomal protein gene expression via PKA and the Forkhead transcription factor FHL1." Cell **119**(7): 969-979.

Matsumoto, K., I. Uno, et al. (1983). "Control of cell division in Saccharomyces cerevisiae mutants defective in adenylate cyclase and cAMP-dependent protein kinase." Exp Cell Res **146**(1): 151-161.

Mazia, D. (1956). "Materials for the biophysical and biochemical study of cell division." Adv Biol Med Phys **4**: 69-118.

Michalewski, M. P., W. Kaczmarski, et al. (1998). "Evidence for phosphorylation of CLN3 protein associated with Batten disease." Biochem Biophys Res Commun **253**(2): 458-462.

Mitsuzawa, H. (1994). "Increases in cell size at START caused by hyperactivation of the cAMP pathway in Saccharomyces cerevisiae." Mol Gen Genet **243**(2): 158-165.

Mortimer, R. K. (1958). "Radiobiological and genetic studies on a polyploid series (haploid to hexaploid) of Saccharomyces cerevisiae." Radiat Res **9**(3): 312-326.

Muller, D., S. Exler, et al. (2003). "Cyclic AMP mediates the cell cycle dynamics of energy metabolism in Saccharomyces cerevisiae." Yeast **20**(4): 351-367.

Mumberg, D., R. Muller, et al. (1995). "Yeast vectors for the controlled expression of heterologous proteins in different genetic backgrounds." Gene **156**(1): 119-122.

Nagai, T., S. Yamada, et al. (2004). "Expanded dynamic range of fluorescent indicators for Ca(2+) by circularly permuted yellow fluorescent proteins." Proc Natl Acad Sci U S A **101**(29): 10554-10559.

Nash, R., G. Tokiwa, et al. (1988). "The WHI1+ gene of Saccharomyces cerevisiae tethers cell division to cell size and is a cyclin homolog." EMBO J **7**(13): 4335-4346.

Nasmyth, K., L. Dirick, et al. (1991). "Some facts and thoughts on cell cycle control in yeast." Cold Spring Harb Symp Quant Biol **56**: 9-20.

Nevoigt, E., J. Kohnke, et al. (2006). "Engineering of promoter replacement cassettes for fine-tuning of gene expression in Saccharomyces cerevisiae." Appl Environ Microbiol **72**(8): 5266-5273.

Paalman, J. W. G., R. Verwaal, et al. (2003). "Trehalose and glycogen accumulation is related to the duration of the G1 phase of Saccharomyces cerevisiae." FEMS Yeast Res **3**(3): 261-268.

Pederson, B. A., C. Cheng, et al. (2000). "Regulation of glycogen synthase. Identification of residues involved in regulation by the allosteric ligand glucose-6-P and by phosphorylation." J Biol Chem **275**(36): 27753-27761.

Pederson, B. A., W. A. Wilson, et al. (2004). "Glycogen synthase sensitivity to glucose-6-P is important for controlling glycogen accumulation in Saccharomyces cerevisiae." J Biol Chem **279**(14): 13764-13768.

Polymenis, M. and E. V. Schmidt (1997). "Coupling of cell division to cell growth by translational control of the G1 cyclin CLN3 in yeast." Genes & Development **11**(19): 2522-2531.

Porro, D., M. Vai, et al. (2009). "Analysis and modeling of growing budding yeast populations at the single cell level." Cytometry A **75**(2): 114-120.

Portela, P., S. Moreno, et al. (2006). "Characterization of yeast pyruvate kinase 1 as a protein kinase A substrate, and specificity of the phosphorylation site sequence in the whole protein." Biochem J **396**(1): 117-126.

Prescott, D. M. (1955). "Relations between cell growth and cell division. I. Reduced weight, cell volume, protein content, and nuclear volume of amoeba proteus from division to division." Exp Cell Res **9**(2): 328-337.

Prescott, D. M. (1956). "Relation between cell growth and cell division. II. The effect of cell size on cell growth rate and generation time in Amoeba proteus." Exp Cell Res **11**(1): 86-94.

Prescott, D. M. (1956). "Relation between cell growth and cell division. III. Changes in nuclear volume and growth rate and prevention of cell division in Amoeba proteus resulting from cytoplasmic amputations." Exp Cell Res **11**(1): 94-98.

Prescott, D. M. (1976). "The cell cycle and the control of cellular reproduction." Adv Genet **18**: 99-177.

Ptacek, J., G. Devgan, et al. (2005). "Global analysis of protein phosphorylation in yeast." Nature.

Reed, S. I. (1980). "The selection of S. cerevisiae mutants defective in the start event of cell division." Genetics **95**(3): 561-577.

Reed, S. I., J. A. Hadwiger, et al. (1985). "Protein kinase activity associated with the product of the yeast cell division cycle gene CDC28." Proc Natl Acad Sci U S A **82**(12): 4055-4059.

Santangelo, G. M. (2006). "Glucose signaling in Saccharomyces cerevisiae." Microbiol Mol Biol Rev **70**(1): 253-282.

Schlee, C., M. Miedl, et al. (2006). "The potential of confocal imaging for measuring physiological changes in brewer's yeast." Journal of the Institute of Brewing **112**(2): 134-147.

Schmelzle, T., T. Beck, et al. (2004). "Activation of the RAS/Cyclic AMP Pathway Suppresses a TOR Deficiency in Yeast." Mol Cell Biol **24**(1): 338.
Schneider, B. L., E. E. Patton, et al. (1998). "Yeast G1 cyclins are unstable in G1 phase." Nature **395**(6697): 86-89.
Schneider, B. L., J. Zhang, et al. (2004). "Growth rate and cell size modulate the synthesis of, and requirement for, G1-phase cyclins at start." Mol Cell Biol **24**(24): 10802-10813.
Searle, J. S. and Y. Sanchez (2004). "Stopped for repairs: a new role for nutrient sensing pathways?" Cell Cycle **3**(7): 865-868.
Silljé, H. H., J. W. Paalman, et al. (1999). "Function of trehalose and glycogen in cell cycle progression and cell viability in Saccharomyces cerevisiae." J Bacteriol **181**(2): 396-400.
Silljé, H. H., E. G. ter Schure, et al. (1997). "Effects of different carbon fluxes on G1 phase duration, cyclin expression, and reserve carbohydrate metabolism in Saccharomyces cerevisiae." J Bacteriol **179**(21): 6560-6565.
Skotheim, J. M., S. Di Talia, et al. (2008). "Positive feedback of G1 cyclins ensures coherent cell cycle entry." Nature **454**(7202): 291-296.
Slater, M. L. (1974). "Recovery of yeast from transient inhibition of DNA synthesis." Nature **247**(439): 275-276.
Spellman, P. T., G. Sherlock, et al. (1998). "Comprehensive identification of cell cycle-regulated genes of the yeast Saccharomyces cerevisiae by microarray hybridization." Mol Biol Cell **9**(12): 3273-3297.
Sudbery, P. E., A. R. Goodey, et al. (1980). "Genes which control cell proliferation in the yeast Saccharomyces cerevisiae." Nature **288**(5789): 401-404.
Swann, M. M. (1957). "The control of cell division; a review. I. General mechanisms." Cancer Res **17**(8): 727-757.
Swann, M. M. (1958). "The control of cell division: a review. II. Special mechanisms." Cancer Res **18**(10): 1118-1160.
Takahata, S., Y. Yu, et al. (2009). "The E2F functional analogue SBF recruits the Rpd3(L) HDAC, via Whi5 and Stb1, and the FACT chromatin reorganizer, to yeast G1 cyclin promoters." EMBO J **28**(21): 3378-3389.
Talia, S. D., J. M. Skotheim, et al. (2007). "The effects of molecular noise and size control on variability in the budding yeast cell cycle." Nature **448**(7156): 947-951.
Tokiwa, G., M. Tyers, et al. (1994). "Inhibition of G1 cyclin activity by the Ras/cAMP pathway in yeast." Nature **371**(6495): 342-345.
Torija, M., M. Novo, et al. (2005). "Glycogen synthesis in the absence of glycogenin in the yeast Saccharomyces cerevisiae." FEBS Letters **579**(18): 3999-4004.
Tu, B. P. and S. L. McKnight (2007). "The yeast metabolic cycle: insights into the life of a eukaryotic cell." Cold Spring Harb Symp Quant Biol **72**: 339-343.
Tyers, M., G. Tokiwa, et al. (1992). "The Cln3-Cdc28 kinase complex of S. cerevisiae is regulated by proteolysis and phosphorylation." EMBO J **11**(5): 1773-1784.
Tyson, C. B., P. G. Lord, et al. (1979). "Dependency of size of Saccharomyces cerevisiae cells on growth rate." J Bacteriol **138**(1): 92-98.
Ubersax, J. A., E. L. Woodbury, et al. (2003). "Targets of the cyclin-dependent kinase Cdk1." Nature **425**(6960): 859-864.

van den Berg, M. A., P. de Jong-Gubbels, et al. (1998). "Transient mRNA responses in chemostat cultures as a method of defining putative regulatory elements: application to genes involved in Saccharomyces cerevisiae acetyl-coenzyme A metabolism." Yeast **14**(12): 1089-1104.

van der Plaat, J. B. (1974). "Cyclic 3',5'-adenosine monophosphate stimulates trehalose degradation in baker's yeast." Biochem Biophys Res Commun **56**(3): 580-587.

Vanoni, M., R. L. Rossi, et al. (2005). "Glucose modulation of cell size in yeast." Biochem Soc Trans **33**(Pt 1): 294-296.

Voth, W. P., J. D. Richards, et al. (2001). "Yeast vectors for integration at the HO locus." Nucleic Acids Res **29**(12): E59-59.

Wagtendonk, W. v. (1955). "Biochemistry and Physiology of Protozoa."

Wang, H., L. B. Carey, et al. (2009). "Recruitment of Cln3 cyclin to promoters controls cell cycle entry via histone deacetylase and other targets." PLoS Biol **7**(9): e1000189.

Wang, H., E. Garí, et al. (2004). "Recruitment of Cdc28 by Whi3 restricts nuclear accumulation of the G1 cyclin-Cdk complex to late G1." EMBO J **23**(1): 180-190.

Wang, Y., M. Pierce, et al. (2004). "Ras and Gpa2 mediate one branch of a redundant glucose signaling pathway in yeast." PLoS Biol **2**(5): E128.

Wapinski, I., A. Pfeffer, et al. (2007). "Natural history and evolutionary principles of gene duplication in fungi." Nature.

Weisz, P. B. (1956). "Experiments on the initiation of division in Stentor coeruleus." Journal of Experimental Zoology **131**(1): 137-162.

Wijnen, H. and B. Futcher (1999). "Genetic analysis of the shared role of CLN3 and BCK2 at the G(1)-S transition in Saccharomyces cerevisiae." Genetics **153**(3): 1131-1143.

Wijnen, H., A. Landman, et al. (2002). "The G(1) cyclin Cln3 promotes cell cycle entry via the transcription factor Swi6." Mol Cell Biol **22**(12): 4402-4418.

Wingender-Drissen, R. and J. Becker (1983). "Regulation of yeast phosphorylase by phosphorylase kinase and cAMP-dependent protein kinase." FEBS Letters **163**(1): 33.

Woldringh, C. L., P. G. Huls, et al. (1993). "Volume growth of daughter and parent cells during the cell cycle of Saccharomyces cerevisiae a/alpha as determined by image cytometry." J Bacteriol **175**(10): 3174-3181.

Zhang, J., Y. Ma, et al. (2001). "Genetically encoded reporters of protein kinase A activity reveal impact of substrate tethering." Proc Natl Acad Sci USA **98**(26): 14997-15002.